Master's Thesis in Graduate School of Library, Information and Media Studies

Soft Manipulator using Lamina Emergent Torsion Array Including Isolated Structure

March 2020

201821607

Miyu Iwafune

Soft Manipulator using Lamina Emergent Torsion Array Including Isolated Structure

Miyu Iwafune

Graduate School of Library,
Information and Media Studies
University of Tsukuba

March 2020

Contents

List of Figures

Chapter 1

Introduction

1.1 Background

Robots have long been developed mainly in the industrial field as machines that do tasks on behalf of humans. Therefore, robots have been required to operate more precisely and to exert a strong force. In order for robots to achieve these requirements, parts such as metal rigid bodies, rigid links, and motors have been used. However, recently, it is expected to utilize robots not only in the factory but also in the service and entertainment industry that is closer to human living space and more variable environments in time. As the property of robots used in such environments, there is a growing demand for new technologies to achieve safety that does not hurt people, and compliance that can flexibly cope with unknown objects and environments.

Recently, in the field of robotics, soft robotics has been actively researched as a robot that combines safety and compliance. Soft robotics realize safety and compliance by developing robots with "softness" in a broad sense, such as soft texture, deformable materials, elastic materials, flexible movements, and softness in friendly and natural interaction with people [1]. Among the research areas of diverse soft robots, this study especially focuses on soft manipulators (robot hands). In the research of soft manipulators, a number of manipulators have been developed, which inspired by biological mechanisms such as human fingers and the legs of mollusks. Soft manipulators consist of soft materials, such as elastomers [2, 3]. Therefore, manipulators have high adaptive ability to unknown objects and environments. For instance, when gripping an unknown object of different shapes and sizes, the manipulator itself can flexibly change shape to fit the object during gripping so that it can be gripped gently without damaging the object. In this way, by creating a manipulator with soft materials, it becomes possible to simplify the compliant operation that had required complicated control to be realized by a conventional rigid manipulator. However, it is difficult to measure the deformed shape of soft material using a conventional sensor, so that there is a problem that is difficult to measure the deformation shape of soft manipulators. Therefore, a number of previous research does not have the function which can measure the deformation shape at a specific time, and the control is carried out by the open-loop. If it is possible to provide a sensing function that can accurately sense the deformation shape of the soft manipulator, it will not only be possible to confirm whether it is operating as controlled, but it will also enable more accurate control by using closed-loop control. In addition, it is expected to have additional functions such as predicting the information of

the gripped object from the soft manipulator's shape.

1.2 Purpose and proposal of this research

The objective of this study is to create a soft manipulator that can accurately sense the deformation state while keeping the compliance which can flexibly correspond even to the unknown object. In order to achieve the objective, in this study, I propose a structure that deforms reversibly from a planar structure to a specific and only one deformation shape.

The proposed structure is compliant for specific and only deformation and rigid for other deformations. In this study, this property regard as "isolation" of deformation. In order to realize the proposed structures, I improve the Lamina emergent torsion array (LETA) structure. The LETA structure is a structure in which curved deformation is realized by cutting of parallel pattern in hard material. However, it is also known that the LETA structure deforms stretching and twisting deformation in addition to the curved deformation. In order to isolate only the curved deformation, the proposed structure is inserted a thin shell structure in the neutral plane of the LETA structure. By creating a soft manipulator using the proposed structure, the deformation shape can be sensed accurately using a flex sensor, which is an element to measure bending. Additionally, since the deformation of the structure is isolated, the proposed manipulator can be driven using a shape memory alloy with simple expansion and contraction movement.

Contributions of this study are as follows.

- Proposal of structure isolated to curved deformation only
- Proposal of a method to create soft manipulators using isolated structures

1.3 Composition of this research

This paper is structured as follows.

Chapter 2 summarizes the related research and describes the standing position of this research. In Section 3, I describe the isolated structure, actuator and sensor, which are the components of the proposed soft manipulator. In addition, the control method of the deformation is also explained. Section 4 confirms the performance of the proposed manipulator through experiments. Section 5 shows examples of applications that can be achieved by using proposed manipulator. Chapter 6 describes future works. Finally, Chapter 7 summarizes this study.

Chapter 2

Related Work

2.1 Manipulator

Manipulator refers to the part of the robot's arms and hands. Manipulators have been developed not only in the field of rigid robotics, which has been developed mainly in the industrial field, but also in the field of soft robotics. In this section, the main material constituting the body of the manipulator is classified into a rigid body, soft body, and hybrid body of rigid and soft, as shown in Figure 2.1. In addition, the previous studies are introduced and the features of each classification are described. In this section, "rigid" refers to materials that do not deform when force is applied, and "soft" refers to materials that deform when force is applied. "Body" refers to any part other than power sources (including electronic components such as sensors in the case of the rigid body).

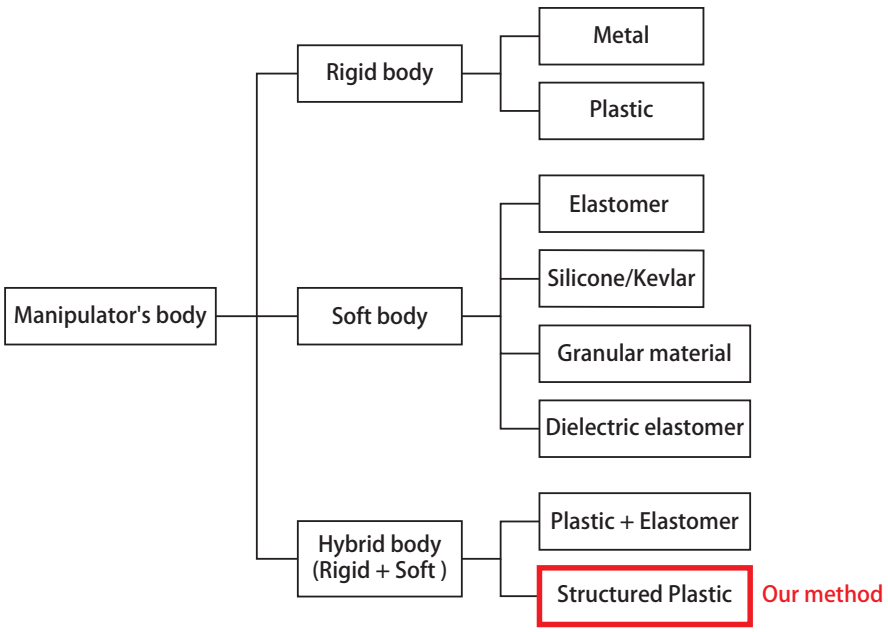

Figure 2.1: Classification of related works.

2.1.1 Manipulator with rigid body

A number of manipulators in industrial fields have consisted of a rigid body. Large robots and arc-welding robots sold by FANUC Co. are manipulators made from a metallic body and servomotors [4]. End effectors (modules at the end of a manipulator that perform operations such as gripping objects) sold by GIMATIC S.r.l. operate by driving a metallic body with a servo motor or pneumatic pressure [5]. There are also rigid body manipulators that can be assembled and used by individuals. UARM SWIFT PRO is a desktop-sized manipulator consisting of metallic bodies and servomotors [6]. MeArm is a manipulator whose cutting data of the body are published as open sources[7]. It can be made by machining plastic rigid plates such as acrylic plates using laser cutter or CNC and assembling them with servo motors.

Manipulators with the rigid body are used in a wide range of areas, from those used in the industrial field to those used in individuals. The rigid body is well suited for precise operation and high power, while the body does not deform and thus require complex control or special mechanisms to achieve compliance.

2.1.2 Manipulator with soft body

Manipulators with soft body have been proposed to realize compliance with a simpler method. In the previous research, manipulators that have soft body using various flexible materials has been proposed. The following describes a manipulator created using flexible material.

Deimel et al. proposed elastomer-made fingers driven by pneumatic expansion [8]. By winding threads around the elastomer with helically, they induce curve deformation during pneumatic expansion. Deimel et al. proposed a elastomer-made hand-type manipulator driven by pneumatic expansion [2]. They also induce curve deformation upon pneumatic expansion by winding the yarn around the silicone in helically. They reproduced the human gripping mode in their's manipulator. Ilievski et al. proposed a starfish-type pneumatic expansion manipulator made from elastomers with differing hardness [9]. Their method induces curve deformation during pneumatic expansion by properly designing the material distribution inside the elastomer structure. Cianchetti et al. proposed a manipulator that drives elastomer using shape memory alloys and cables [10]. Their manipulator is inspired by the tentacle of octopus. They induced the elastomer skin to the curve deformation by expanding and contracting the shape memory alloys and cables. Jin et al. and Rodrigue et al. proposed a soft manipulator with shape memory alloys embedded inside elastomer [11, 12]. They induced curved deformation by contracting the inside the neutral plane of the rectangular parallelepiped elastomer with SMA. Shepherd et al. proposed a pneumatic expansion manipulator that is more puncture-resistant than elastomer-made manipulators by using elastomer-Kevlar composites [13]. Their method induced curve deformation during pneumatic expansion by using a bellows structure. Brown et al. proposed a soft manipulator using granular material [14]. They proposed a universal gripper that can grip an object of any shape or surface material using jamming transition phenomenon of granular material (a phenomenon in which a bag containing granular material is soft under normal conditions, but granular material becomes hard when air is removed from the bag). Cheng et al. proposed using jamming transition phenomena at the joints of soft manipulators[3].

Shintake et al. proposed a soft manipulator using dielectric elastomers that bending when applied with voltages and electrostatically attach [15].

Manipulators with the soft body have been proposed with various kinds of flexible materials and driving methods to suit the properties of the materials. Because of the high flexibility, the soft body can change the shape of the manipulator itself to suit any object shape even under uncontrolled conditions, and cope with disturbances without being broken. On the other hand, because of high flexibility, there is a problem that it is difficult to sense a specific deformation shape of a specific time of the manipulator itself. Therefore, in a number of previous researches, the deformation is controlled by open-loop without carrying out the sensing. In the previous research of soft manipulators and soft robotics, there are several studies in which shape estimation is performed using an externally installed camera. However, this greatly restricts the range of movement and the operating environment [16, 17]. Research on flexible sensors that can measure deformation is also being conducted, but most of the research is mainly conducted as a sensor alone [18, 19, 20]. Although there are several previous research is embedded flexible sensors in soft bodies and sensing the deformation shape of the manipulator itself, it is assumed that there is no deformation by disturbance [21, 22].

2.1.3 Manipulators with hybrid body of rigid and soft

It is important to accurately measure the deformation state of the manipulator in order to confirm whether it operates as controlled and to enable more accurate control by using closed-loop control. However, the manipulators with soft body proposed in the previous research had a problem that the deformation state is difficult to measure because the manipulator itself is deformed irregularly. In order to solve this problem, methods have been proposed that are using a hybrid body of rigid and soft and constraining the direction of deformation.

Homberg et al. proposed a technique to embed a constrained layer that restricts the direction of bending in an elastomer-made manipulator driven by pneumatic expansion [23]. By uniquely determining the bending direction, the bending shape was made measurable with a flex sensor that measures the bending commercially available. They used the Lamina Emergent Torsion Array (LETA) structure as the constraining layer. LETA is a structure in which curved deformation is realized by putting a cut pattern of parallel in hard material. However, the paper by Ohshima et al. shows that the LETA structure has four deformations modes (Bending in-plane mode (BIP-mode), Bending out-of-plane mode (BOP-mode), Stretching mode (S-mode), Twisting mode (T-mode)) that are shown in Figure 3.1 [24]. Therefore, it is suggested that the manipulator proposed by Homberg et al. may deform into unintentional modes other than the BOP-mode they assumed when an external force is applied, and the deformation shape may not be sensed correctly.

2.2 Material whose deformation is controlled by the design of the structure

Artificial materials, such as the LETA structure described in Section 2.3, have mechanical properties that are not originally possessed by the base material in the proper design of

the structure. These materials have been studied in the architectural field and the material engineering field. In particular, these studies have been more active in recent years because the generalization of 3D printers and laser cutters has progressed and the realization of complex structures has become simpler. In the following, I introduce a previous study in which deformation is controlled by appropriately designing the structure of a single material.

Panetta et al. proposed a method to induce the desired deformation during compression by optimizing density distributions in objects using microstructures [25]. Schumacher et al. and Martinez et al. proposed a method to induce the desired deformation by optimizing density distributions in arbitrary solid shapes using microstructures [26, 27]. Iron et al. proposed a method of designing a structure that performs the desired operation by designing the inside of an object using several kinds of microstructures [28, 29]. Fillipov et al. propose a structure that utilizes a Miura-ori, which is one of folding methods of origami, and expands the folded structure to the desired shape at once when an external force is applied in the expansion direction from the folded state [30].

The re-entrant honeycomb structure can be realized negative Poisson's ratio and positive Poisson's ratio by changing the bond angles between the local beams. Poisson's ratio is the ratio of the strain generated along the direction of the force to the strain generated in the direction perpendicular to the force when the force is applied to an object. In other words, when the structure is designed so that the Poisson's ratio of the object becomes negative, it is deformed out-of-plane to the dome type, and when the structure is designed so that the Poisson's ratio becomes positive, it is deformed out-of-plane to the saddle type [31, 32, 18]. However, the re-entrant honeycomb structures are also known to deform other than the out-of-plane deformation described above. Therefore, Ohshima et al. showed that the re-entrant honeycomb structure can suppress deformation other than dome-type or saddle-type by adding box spring structures to the re-entrant honeycomb structure [33].

2.3 Position of this study

In this study, by inserting a thin shell into the LETA structure, I propose an isolated structure that is flexible only in the intended one deformation mode (curved deformation) but stiff in the other deformation modes. The proposed structure can be used as a hybrid body with a soft body-like behavior with compliance for a flexible one-deformation mode and a rigid body-like behavior without deformation for other deformations. By using the proposed structure, the deformation shape can be accurately measured even in the sensing by the flex sensor, because the deformation mode is not deformed except for the intended deformation mode when an external force is applied to the soft manipulator.

Chapter 3

Soft manipulator of proposed method

3.1 Isolated structure

3.1.1 Lamina Emergent Torsion Array

In this study, Lamina Emergent Torsion Array (LETA) structure is used as a structure to realize the curved deformation. LETA is a structure in which curved deformation is realized by putting a cut pattern of parallel in hard material. LETA structure is sometimes referred to as Lamina Emergent Array [34], Array of LET joint [35], Compliant arrays [34], slit-based material [24], but in this paper I refer to it as LETA structure. As examples using LETA structure, wooden interiors and furniture with beautiful curved surfaces have been proposed [36]. LETA structures are also being studied in the fields of materials engineering and architecture. Lamina Emergent Mechanisms (LEMs) is a superordinate concept of LETA structure. LEMs a mechanical joint material that realizes out- of- plane deformation by utilizing the deflection of members from a plane [37]. There are the following advantages compared LEMs to conventional mechanical joints such as pin joints and cams.

- Reduced number of parts
- Lack of contact friction
- Compact size (ex. Can be transported on a flat surface and deployed where necessary)
- Can be scaled to micro-level

Because of these advantages, analysis of the structure and research on the modeling technique are advancing [37]. In particular, with regard to LETA, Nelson et al. proposed a design method of LETA's cutting pattern in order to design a desired developable structure. As shown in the paper of Nelson et al., by providing offsets to the cutline (ruling line), not only the curve deformation but also the LETA structure can be curl deformed [34]. Ohshima et al. classified the deformation mode of the LETA into four (Bending in-plane mode (BIP-mode), Bending-out-of plane mode (BOP-mode), Stretching mode (S-mode) and Twisting mode (T-mode)) shown in Figure 3.1, and proposed the stiffness function for each deformation [24]. From the study by Ohshima et al., we can derive how much each structural parameter contributes to the stiffness of each deformation. In other words, it

is suggested that the isolation of deformation, which is the purpose of this section, may be theoretically achieved by properly designing the structural parameters (the thickness of local beams, the width of local beams, the length of local beams, the number of the local beams, etc) in the stiffness model. However, it is difficult in actual manufacturing to realize isolate of deformation with a small structure of centimeter-scale, because isolation by this method is greatly influenced by the resolution of manufacturing equipment. Therefore, in this study, instead of designing parameters appropriately, I propose a method to realize simpler and stronger isolation by using a thin shell structure. Details of the technique are given in the next subsection. In the following subsection, I propose a method to isolate a single deformation using N=1 (Figure3.2) structures with the lowest stiffness for each deformation in the LETA structure.

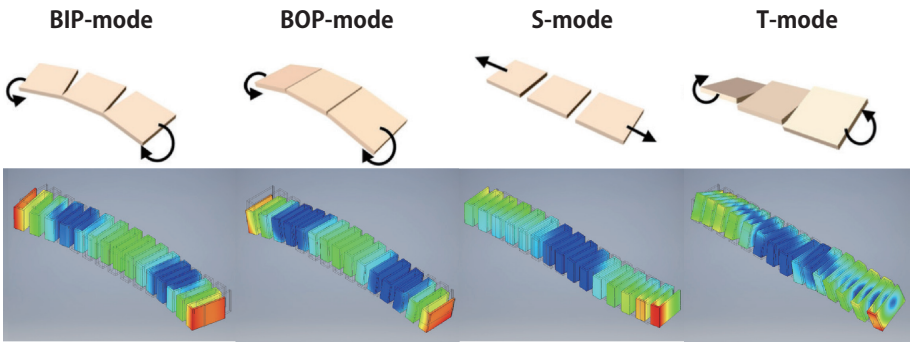

Figure 3.1: Deformation modes of LETA.

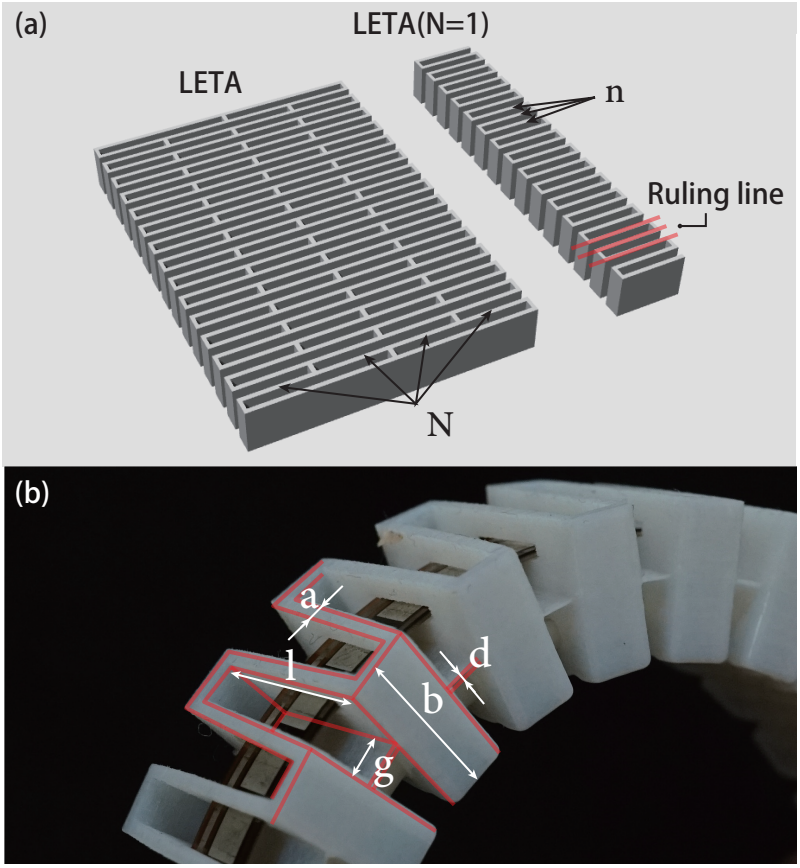

Figure 3.2: Parameter of the following Structure, (a)LETA and LETA(N=1), (b)Proposed structure.

3.1.2 Design method of isolated structure

In this study, I propose to insert a thin shell into the neutral plane of LETA (N=1) structure in order to isolate LETA (N=1) structure with originally four deformation modes into one deformation mode. By inserting a thin shell which is easily warping into the neutral plane of the LETA (N=1) structure, the stiffness of the deformation other than the warping direction of the shell can be increased. In this method, as shown in Figure 3.3, by changing the direction in which the thin shell is inserted, it is possible to create a structure in which only the bending deformation of BOP-mode or BIP-mode is isolated.

Each parameter of the proposed structure is shown in Figure 3.2. "a" is the thickness of the local beam, "l" is the length of the local beam, "g" is the distance between the local beam, "b" is the thickness of the structures, "d" is the thickness of the thin shell, "n" is the number of local beam, "θ" is the offset angle of the ruling line.

In this study, I have modeled the traditional LETA (N=1) structure, the isolated BOP-mode ($\theta = 0°$) structure, the isolated BIP-mode ($\theta = 0°$) structure, the isolated BOP-mode ($\theta = 30°$) structure, and the isolated BOP-mode ($\theta = 45°$) structure (Figure3.3, 3.8), and evaluated the isolation property of each structure in the next subsection.

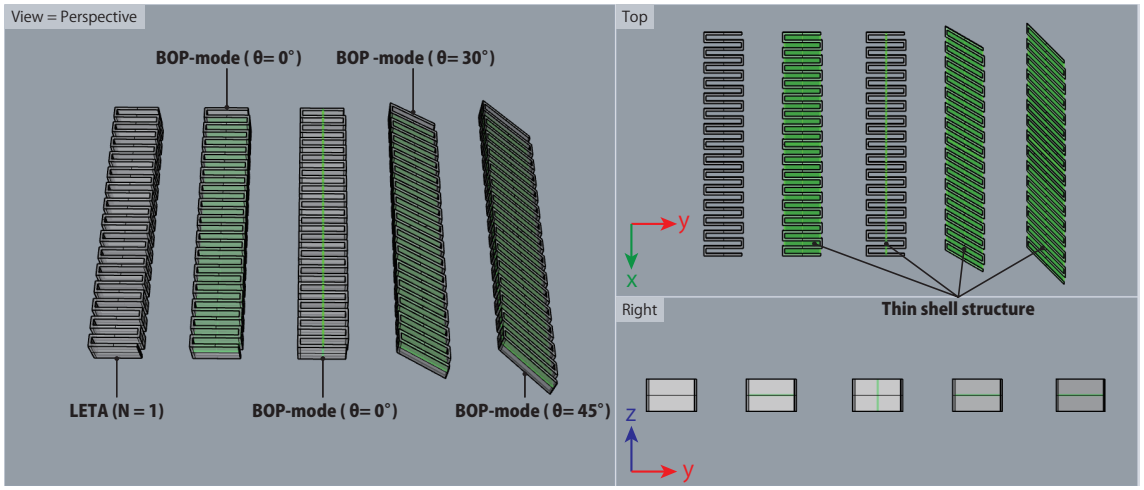

Figure 3.3: Conventional structure (LETA(N=1)) and isolated structures (isolated BOP-mode ($\theta = 0°$), isolated BIP-mode($\theta = 0°$), isolated BOP-mode($\theta = 30°$), isolated BOP-mode($\theta = 30°$)).

3.1.3 Evaluation of isolated structure

In this section, eigenvalue analysis is performed to evaluate that the deformation of the proposed structures is isolated (see the technique of Fillip et al. [30]). By comparing the eigenvalue analysis results of the conventional LETA (N=1) structure and the proposed structure, it is shown that the proposed structure is isolated. In the following, the theory of eigenvalue analysis, evaluation technique of isolation, analytical conditions are shown, and actual analytical results are shown.

3.1.3.1 Evaluation method

Eigenvalue analysis is carried out as a method of evaluating isolation. The theory of eigenvalue analysis is described below [38].

Eigenvalue analysis is a kind of vibration analysis. The equation of motion of a multi-degree of freedom system is,

$$[M]\{\ddot{x}\} + [C]\{\dot{x}\} + [K]\{x\} = \{F\}, \tag{3.1}$$

where $[M]$ is the overall mass matrix, $[C]$ is the overall damping matrix, $[K]$ is the overall stiffness matrix, $\{x\}$ is the overall displacement vector, and $\{F\}$ is the overall load vector. In eigenvalue analysis, $[M]$, $[C]$, and $[K]$ are constant matrices that do not change over time.

Since the eigenvalue analysis evaluates the free vibration characteristics neglecting damping and load, it becomes $[C] = 0, \{f\} = 0$, and the Equation 3.1,

$$[M]\{\ddot{x}\} + [K]\{x\} = 0. \tag{3.2}$$

Since the solution of the equation of motion Equation 3.2 is assumed to be simple harmonic oscillation, the total displacement vector $\{x\}$,

$$\{x\} = Acos\omega t + Bsin\omega t, \tag{3.3}$$

where A and B are arbitrary constants,ω is angular velocity, and t is time. The first and second derivatives of Equation 3.3 is below.

$$\{\dot{x}\} = -A\omega sin\omega t + B\omega cos\omega t \tag{3.4}$$

$$\{\ddot{x}\} = -A\omega^2 cos\omega t - B\omega^2 sin\omega t = -\omega^2\{x\}. \tag{3.5}$$

Equation 3.3 and Equation 3.5 are substituted for Equation 3.2 and simplified is below.

$$([K] - \omega^2[M])\{x\} = 0. \tag{3.6}$$

Equation 3.6 is referred to as an expression for an eigenvalue problem. It is an eigenvalue analysis to obtain ω^2 and ϕ which satisfies this formula. Where ω^2 is the eigenvalue, ϕ is the eigenvector, and the eigenvector corresponds to the deformed mode.

Equation 3.3 is a general solution of simple harmonic oscillation, and the angular acceleration is expressed as follows using the spring constant k and the mass m.

$$\omega = \sqrt{\frac{k}{m}} \tag{3.7}$$

The angular acceleration is converted to frequency as below.

$$f = \frac{1}{2\pi}\sqrt{\frac{k}{m}} \tag{3.8}$$

Since the spring constant k is a constant indicating the stiffness of the analyzed object, from Equation 3.8, the frequency f is proportional to the square of the spring constant k. In other words, the lower the frequency, the lower the stiffness to the corresponding eigenmode, indicating that it is easy to deform. Using the relationship between this frequency and stiffness, it is confirmed that the deformation of the proposed structure is isolated.

3.1.3.2 Analysis conditions

Five structures shown in Figure3.3 are used for the analysis. The parameters of each structure are shown in Table 3.1.

Eigenvalue analysis is carried out using the Autodesk Inventor. The analysis is carried out without considering the boundary conditions. In this case, since the first six eigenmodes represent the rigid motion (movement and rotation in the axial direction of each of the x, y, and z axes) in a three-dimensional space, the natural frequency is 0. Therefore, I omit the first six eigenmodes. The average element size of the mesh (the size of the element when the analysis model's size is assumed to be 1) is 0.08. The material properties used in the analysis were the parameters of ABS resins that had been predefined in the Inventor. Because, from the standpoint of isolation, ABS-resin, PLA-resin, and photocuring-resin that can be manufactured by 3D printers do not produce large differences, I used the material properties of ABS resin this time. The material properties of ABS-resin are shown in table 3.2.

As a criterion for the isolation in this study, it is assumed that the frequencies of the deformed modes to be induced are well isolated when it is larger than four times the frequencies of the other deformed modes.

Table 3.1: Parameters of structures that are analyzed.

	LEAT(N=1)	**Isolated BOP** (θ **=0** $^\circ$)	**Isolated BIP** (θ **=0** $^\circ$)	**Isolated BOP** (θ **=30** $^\circ$)	**Isolated BOP** (θ **=45** $^\circ$)
a	0.80 [mm]	0.80 [mm]	0.80 [mm]	0.80 [mm]	0.80 [mm]
l	14.00 [mm]	14.00 [mm]	14.00 [mm]	14.00 [mm]	14.00 [mm]
g	3.0 0[mm]	3.0 0[mm]	3.0 0[mm]	3.0 0[mm]	3.0 0[mm]
b	10.00 [mm]	10.00 [mm]	10.00 [mm]	10.00 [mm]	10.00 [mm]
d	-	0.25 [mm]	0.25 [mm]	0.25 [mm]	0.25 [mm]
n	30	30	30	30	30
θ	0 [$^\circ$]	0 [$^\circ$]	0 [$^\circ$]	30 [$^\circ$]	45 [$^\circ$]

Table 3.2: The material properties of ABS-resin.

Behavior	isotropy
Young's modulus	2.240 [GPa]
Poisson's ratio	0.38
Elastic shear modulus	805.000 [MPa]
Density	1.060 [g/cm^3]
Yield strength	20.000 [MPa]
Tensile strength	29.600 [MPa]

3.1.3.3 Analysis result

The results of the eigenvalue analysis of each structure shown in Figure 3.3 are shown in Figure 3.4. Conventional LETA (N=1) structure has relatively low frequencies for four eigenmodes. In particular, the differences in the frequencies of the lower natural frequency BIP-mode (32.78[Hz]) and BOP-mode (50.68[Hz]) are less than four times, and the structures are not isolated. On the other hand, Isolated BOP-mode structure can be said that the frequency (50.72 [Hz]) of the deformation of the BOP-mode is sufficiently low compared with the frequency of the other three deformations, and is isolated in BOP-mode. Similarly, Isolated BIP-mode structure showed that the frequency (78.93[Hz]) of the deformation of the BIP-mode was sufficiently low compared with the frequency of the other three deformations, indicating that it was isolated in BIP-mode.

Eigenvalue analysis was also carried out for structures in which angles of the ruling line are non zero. As shown in Figure 3.5, both structures of isolated BOP-mode ($\theta = 30$) and isolated BOP-mode ($\theta = 45$) are sufficiently low in frequencies of BOP-mode deformation and can be said to be isolated in BOP-mode.

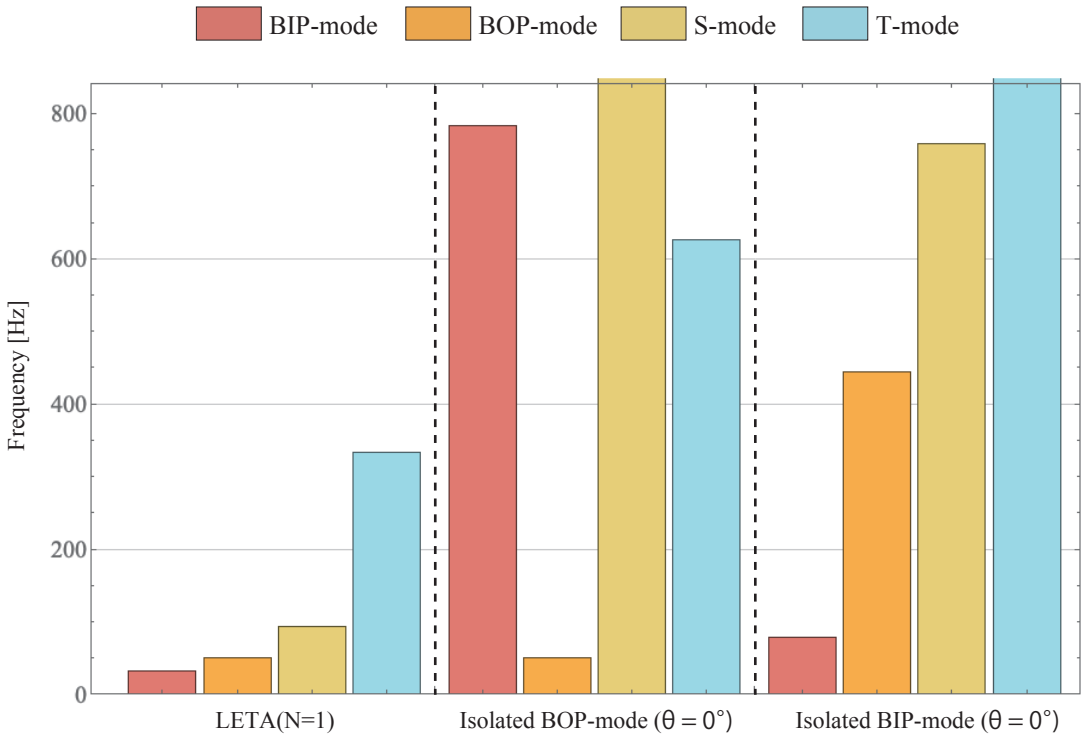

Figure 3.4: Result of eigenvalue analysis (LETA(N=1), Isolated BOP-mode, Isolated BIP-mode).

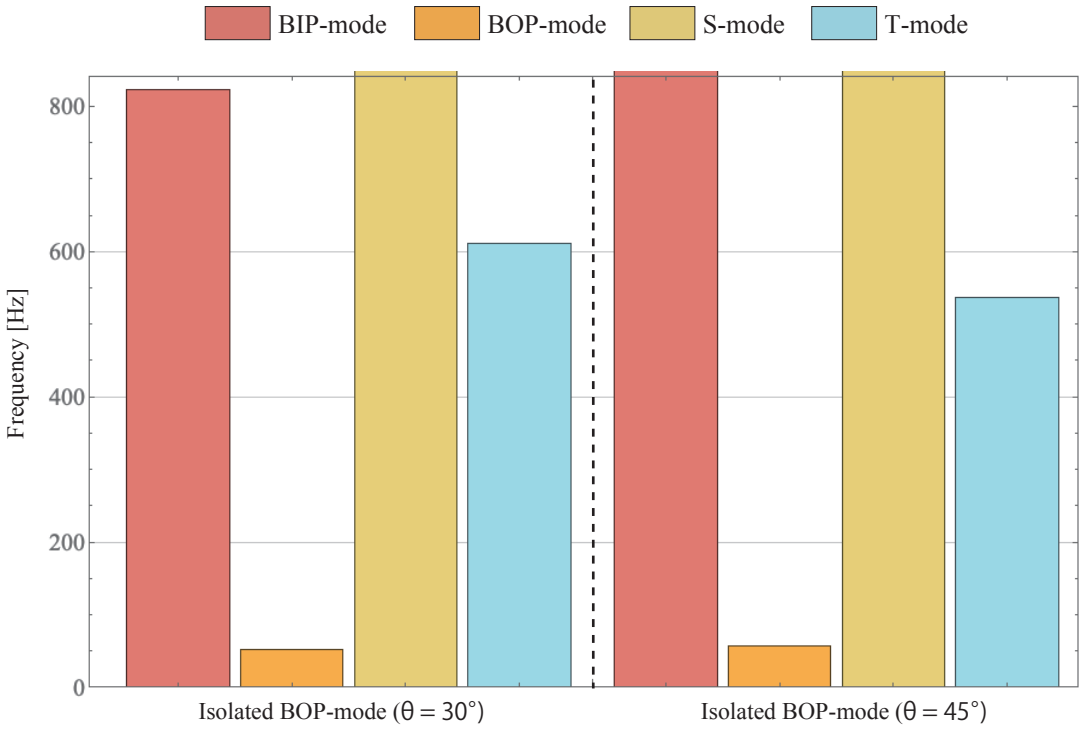

Figure 3.5: Result of eigenvalue analysis.

3.1.4 Fabrication of Isolated Structures

In this section, I describe the fabrication method of the proposed structure. Conventionally, a number of LETA structures were made by cutting rigid panels with cutting equipment such as laser cutters. On the other hand, proposed structures have a thin shell inside the LETA structure, and it can not be processed by a laser cutter. Therefore, it was manufactured using a 3D printer.

In order to confirm whether the manufactured structures deform as designed, simulations of deformation were made using CAD software (Rhinoceros, Grasshopper) and compared with the manufactured structures. The simulation made in this study simulates the deformation of the neutral plane of the structure. In order to simulate the deformation theoretically, simulations are carried out by ignoring the effect of thickness.

Figure 3.6, 3.7, 3.8, 3.9 shows the result of deformation simulation of each structure shown by Figure 3.3 and comparison with the structure actually produced. The fabricated structure was deformed by pulling with a thread. It can be seen from Figure 3.6, 3.7, 3.8, 3.9 that it is deformed consistent with the simulation.

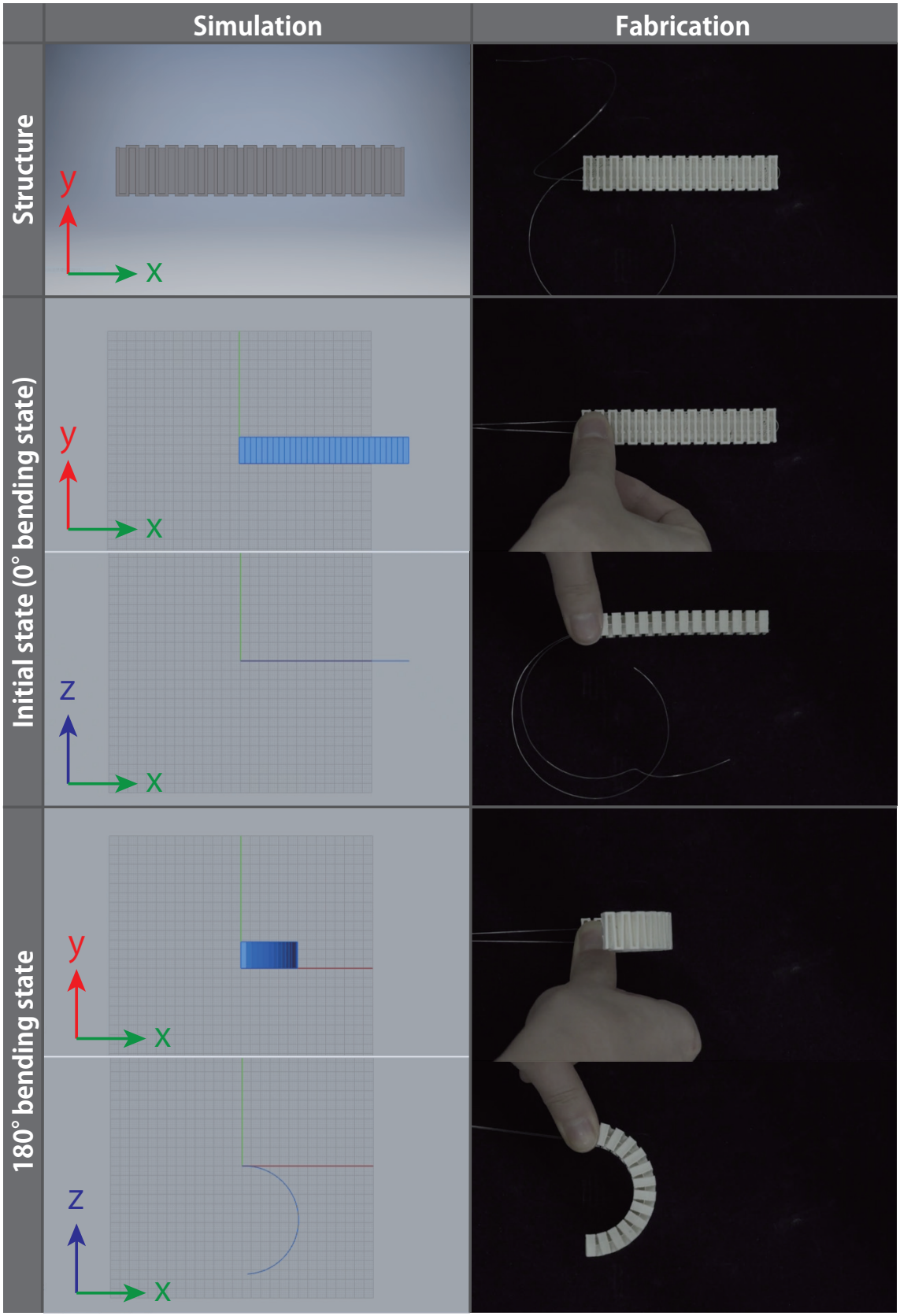

Figure 3.6: Deformation result of isolated BOP-mode($\theta = 0°$) structure.

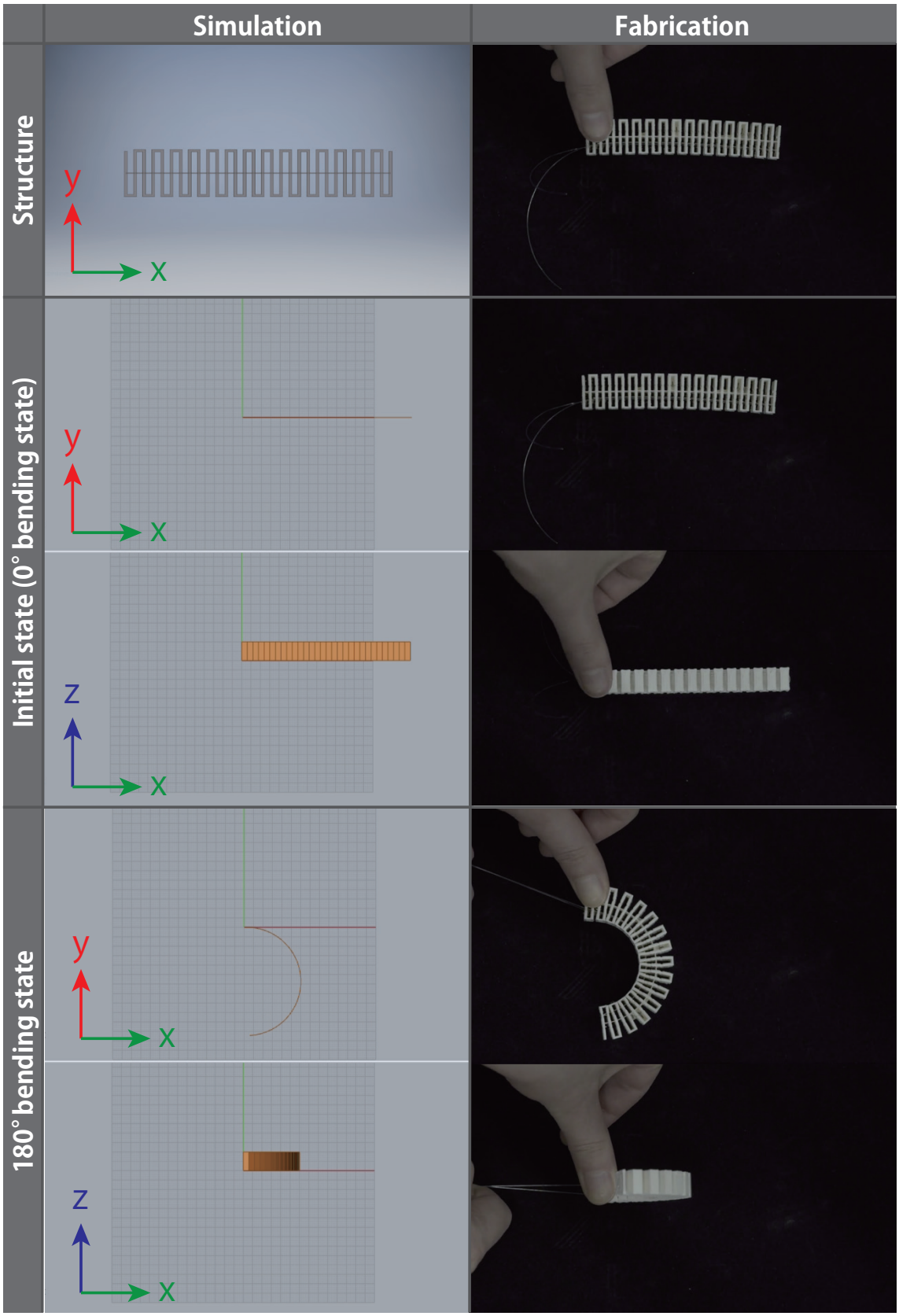

Figure 3.7: Deformation result of isolated BIP-mode($\theta = 0°$) structure.

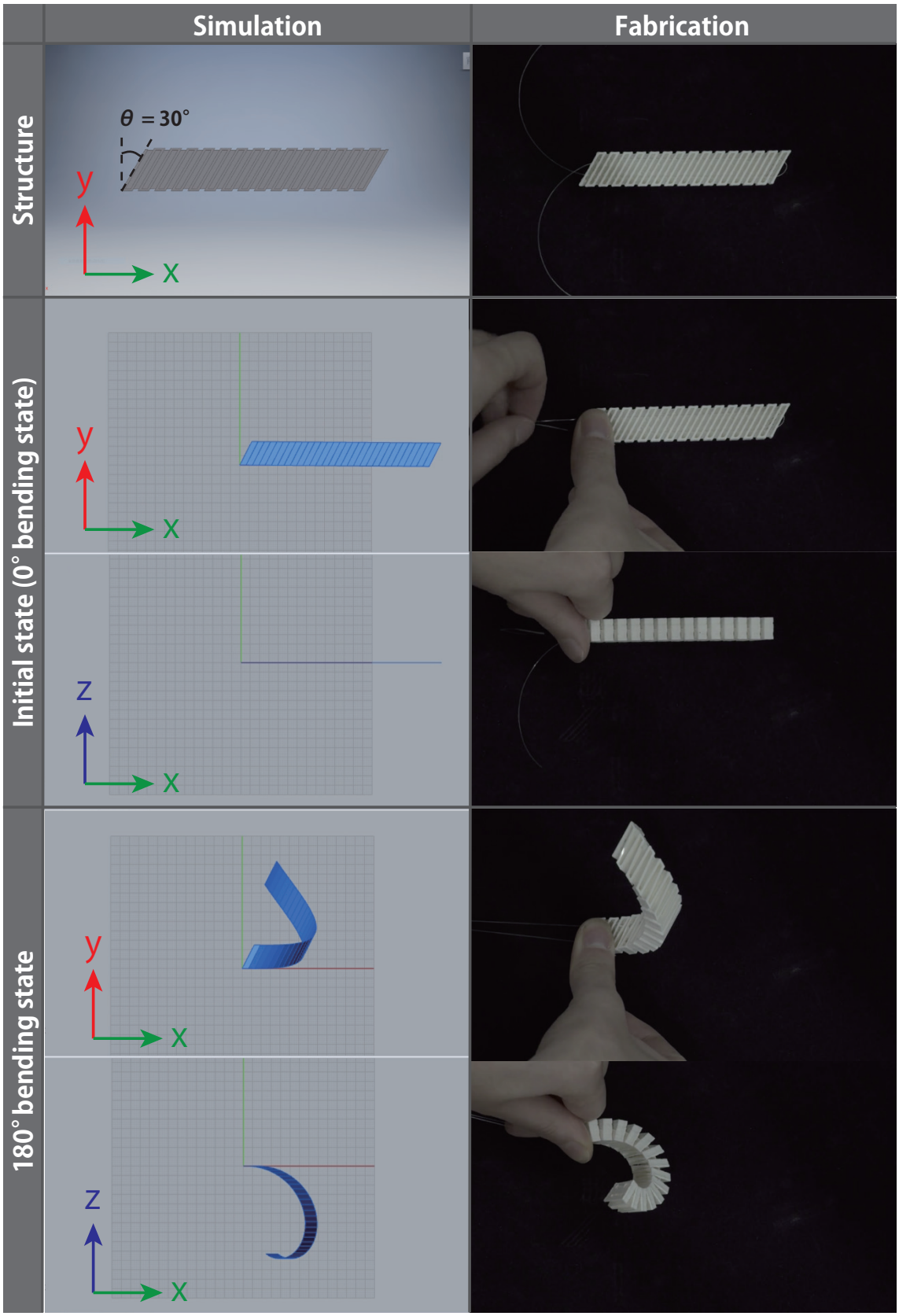

Figure 3.8: Deformation result of isolated BOP-mode($\theta = 30°$) structure.

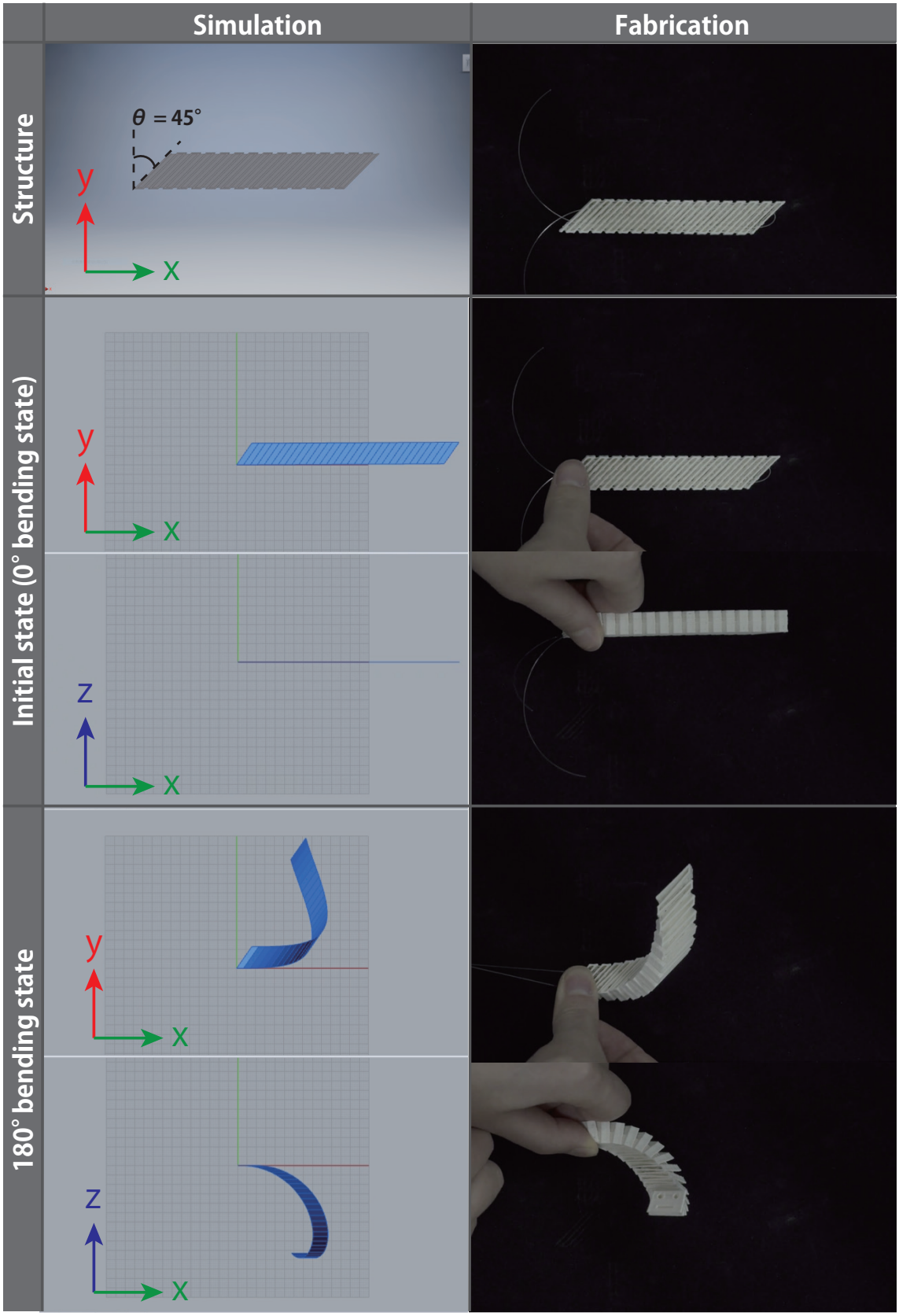

Figure 3.9: Deformation result of isolated BOP-mode($\theta = 45°$) structure.

3.2 Actuator

The main idea for actuating the proposed structures is to change the geometric distances. On the developable surface, the distance does not change during deformation because the thickness is assumed to be negligibly thin enough. On the other hand, the proposed structure has a finite thickness, so that the distances change during deformation. As shown in Figure 3.10, the distance of the neutral plane does not change, but the distance extends at the upper side of the neutral plane and the distance shrinks at the lower side of the neutral plane. Using this characteristic, the proposed structures is driven by reducing the distance on the lower side of the neutral plane using a linear actuator.

As a linear actuator that reduces the distance, the shape memory alloy (SMA) is utilized in this study. SMA is an alloy that has the property of returning to its original shape when heated at temperatures above the transformation point even if it is deformed under temperatures below the transformation point. SMA is also characterized by no vibration or driving noise during driving. In this study, I utilized Bio Metal Helix 150 (BMX) [39], which is coil-shaped and has outstanding contractility among SMAs. The performance of BMX is shown in Table3.3. The BMX is a small and flexible actuator with a diameter of 0.62mm, thus BMX can be inserted inside the proposed structures.

The BMX contract to the original length by heating (Figure3.11). In this study, the coil is heated by applying current, which is one of the methods proposed by the seller. In order to prevent plastic deformation and melting of the proposed structure due to heat generated by BMX, insert BMX into the structure after passing it through a silicon tube (Figure3.12). BMX is inserted into the structure in a state where it is 50% extension from its original length in advance.

Table 3.3: The performance of BMX.

Standard coil diameter	0.62 [mm]
Practical maximum force produced	20 to 40 [gf]
Kinetic displacement	50 [%]
Standard drive current	0.2 to 0.3 [A]
Standard electric resistance	400 [Ω/m]
Allowable upper temperature limit	50 to 60 [°C]
Service life	100,000 [times]

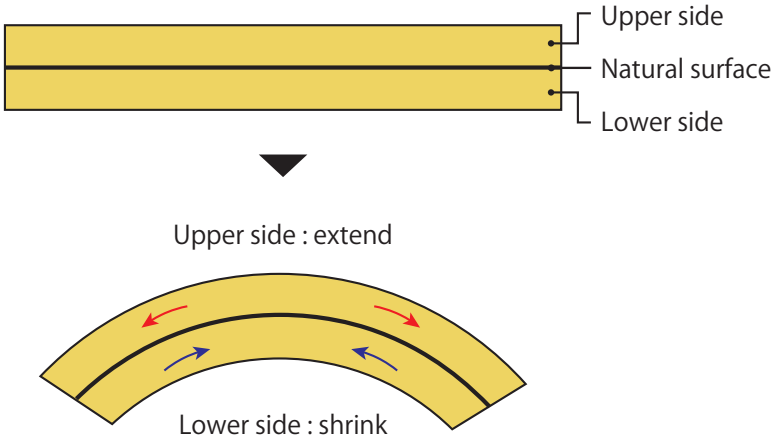

Figure 3.10: Upper and lower side deformation of the neutral plane.

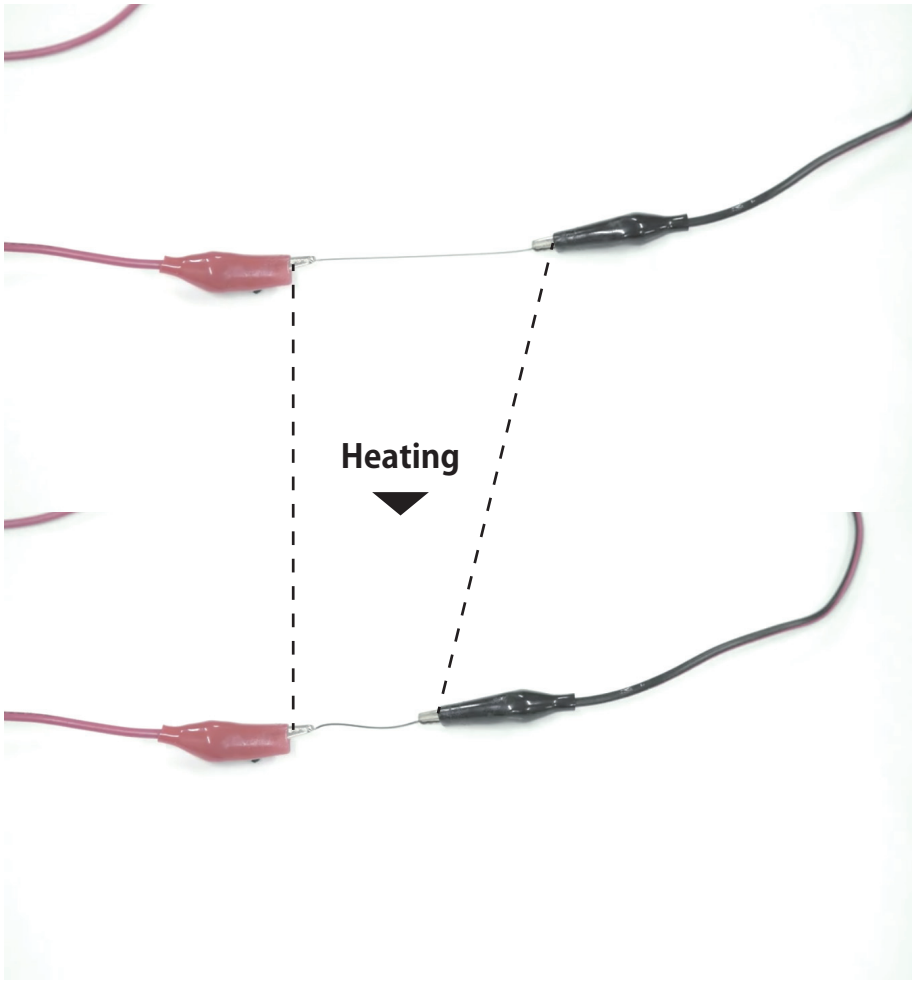

Figure 3.11: Deformation of BMX.

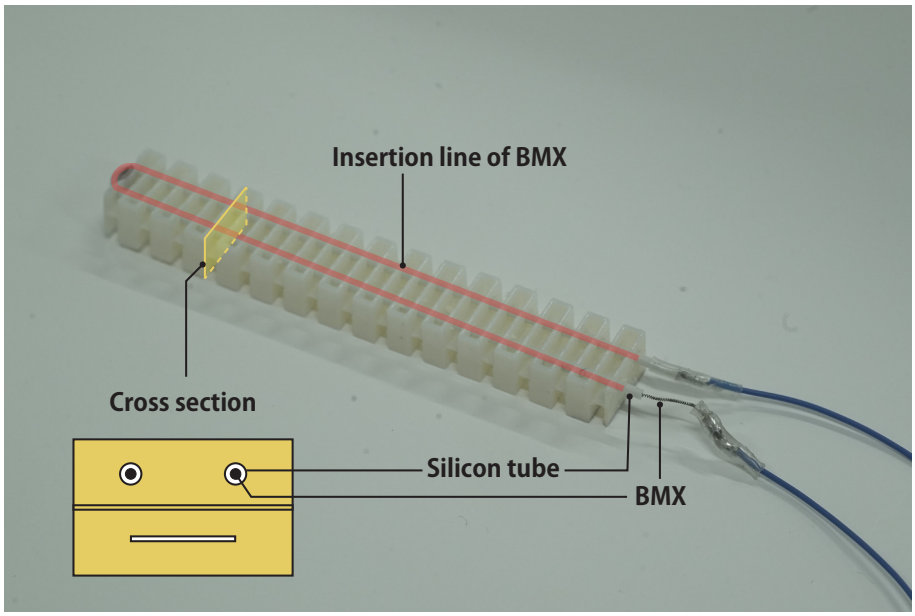

Figure 3.12: BMX inserted into proposed manipulator.

3.3 Sensor

The flex sensor was adopted in this study as a technique for measuring the deformation state of the structure (Figure3.13). The flex sensor measures the displacement of the structure by measuring the change in the resistance value generated by the metal on the sensor surface stretches (shrinks) due to the application of an external force(Figure3.14). Because the flex sensor has a thin plate structure, it has the flexibility of multiple degrees of freedom. However, since the deformation shape of the proposed structure is determined uniquely in advance, the sensing value of the flex sensor and the deformation state of the proposed soft manipulator can be matched one-to-one. In this study, the spectra symbol's flex sensor [40] is used as a flex sensor by cutting it according to the length of the proposed structure. In the case of cutting, in order to disconnect at the cut portion, the connection is made by using solder and swage. The performance of the flex sensor is shown in Table 3.4. Figure 3.15 shows the flex sensor inserted inside the proposed structure.

Table 3.4: The performance of flex sensor.

Life cycle	1,000,000 [times]
Temperature range	-35 to +80 [° C]

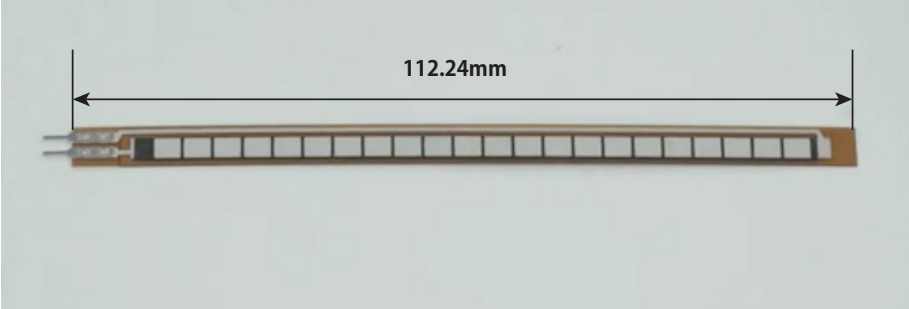

Figure 3.13: Flex sensor.

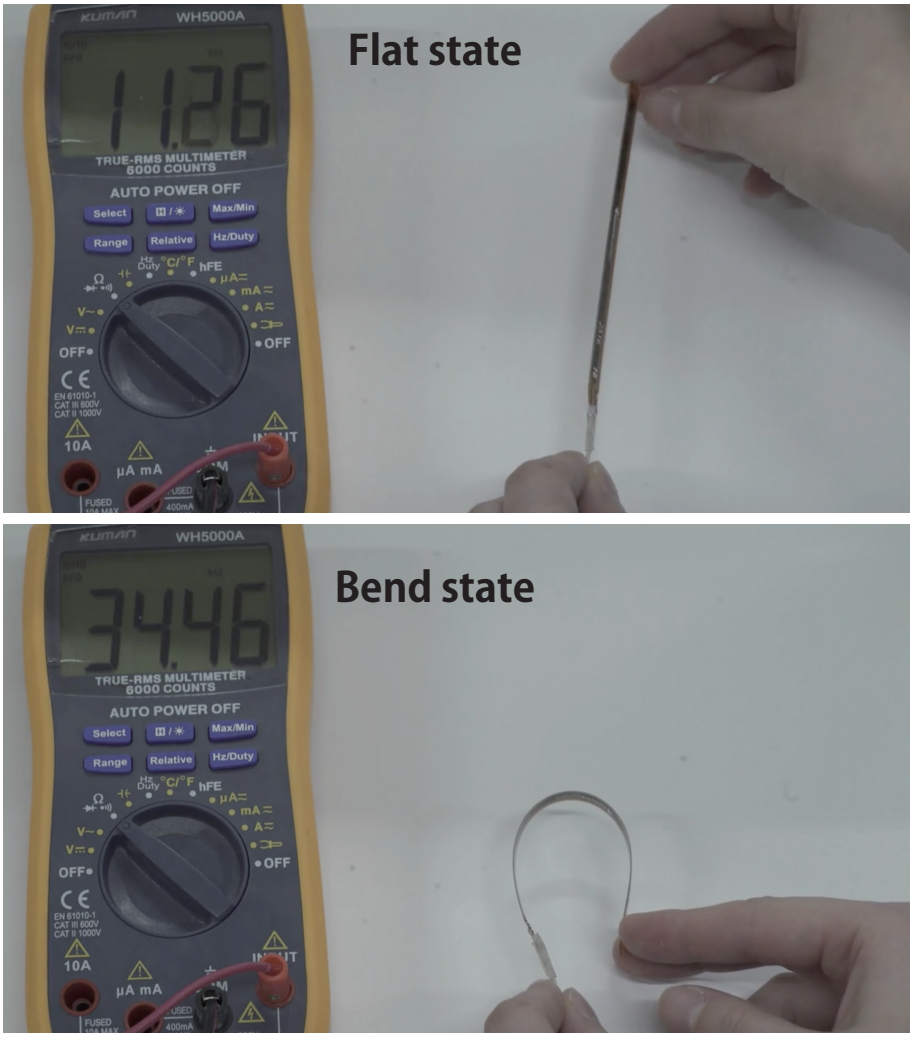

Figure 3.14: Change in the resistance value of flex sensor.

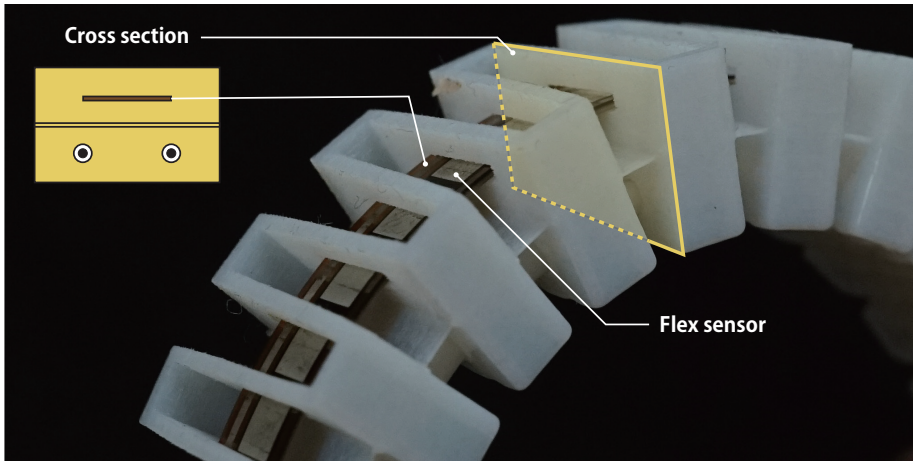

Figure 3.15: Flex sensor inserted into proposed manipulator.

3.4 Manipulation Method

The proposed soft manipulator performs the deformation of the desired deformation modes by applying a current to the BMX and reducing the distances below the neutral plane of the structure. In the case the output control of the current is not performed, the proposed soft manipulator has two stable states; the initial state in which no current flows and, the equilibrium state in which the elastic energy of the structure and the maximum output of the BMX are balanced (Figure4.2). The case that the output control of the current is not performed is called ON / OFF control. In order to hold the deformation in any state between the two stable deformation states, it is necessary to control the output of the current. Therefore, in this study, PID control is applied as a method of output control of the current. PID control is a feedback control technique that controls the input value so that the difference (control deviation) between the current output value and the target value becomes small. In the case of this study, the amount of input current is controlled so that the difference between the target value and the current sensor value is small, with the sensor value in the desired deformation state as the target value.

In PID control, the manipulated variable input to the system is the sum of the amount proportional to the control deviation, the amount obtained by integrating the control deviation, and the amount obtained by differentiating the control deviation. The input value is express as below.

$$u(t) = K_p e(t) + K_i \int_0^t e(\tau)d\tau + K_d \frac{de(t)}{dt},$$

where u(t) is the manipulated variable (the amount of input current to the system) and e(t) is the control deviation (the difference between the target value and the current value). In addition, K_p denotes proportional gain, K_i denotes integral gain, and K_d denotes differential gain. Figure3.16 shows the pipeline of this system. As shown in the diagram, the data-processing was performed using Arduino Uno. Sensor values were acquired at 0.1s intervals and reflected in the operation amount.

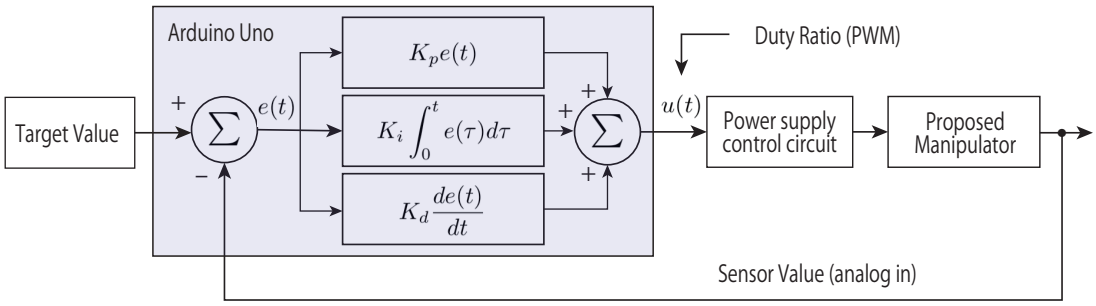

Figure 3.16: Brock diagram of PID control.

Chapter 4

Experiment

4.1 Experiment1: Evaluation of isolated structure

4.1.1 Purpose

As described in Section 3.1.2, the proposed structures are isolated by inserting the thin shell in the LETA(N=1) structure. In Section 3.1.3, I carried out the eigenvalue analysis to evaluate the isolation of structures. In this section, uniaxial load experiments are conducted to confirm that the proposed structure is isolated even in the real environment.

4.1.2 Evaluation conditions

Evaluative experiments are carried out for two structures; LETA(N=1) structure and isolated BOP-mode structure. The structural parameters of the LETA (N=1) structure are 0.8mm in the thickness of the local beam, 14mm in the length of the local beam, 3mm in distance between the local beam, 10mm in the thickness of the structures, and 30 in a number of local beams. The structural parameters of the Isolated BOP-mode structure are 0.8mm in the thickness of the local beam, 14mm in the length of the local beam, 3mm in distance between the local beam, 10mm in the thickness of the structures, 0.25mm in shell thickness, and 30 in the local beams.

In this evaluation experiment, the experiment was carried out for three deformation modes except for the twisting, because it is difficult to realize T-mode in real environmental. As a method of uniaxial load experiment, weight is suspended at the tip of the structures. A load of 20g was applied to the BOP-mode and the BIP-mode, and a load of 40g was applied to the S-mode which is stiffer than BOP-mode and BIP-mode.

4.1.3 Result

As shown in Figure 4.1, the LETA (N=1) structure is deformed for all three deformation modes. On the other hand, as shown in Figure 4.1 it can be seen that the Isolated BOP-mode structure is deformed only BOP-mode. From this result, it was confirmed that the structure was isolated by adding the thin shell to LETA (N=1) structure.

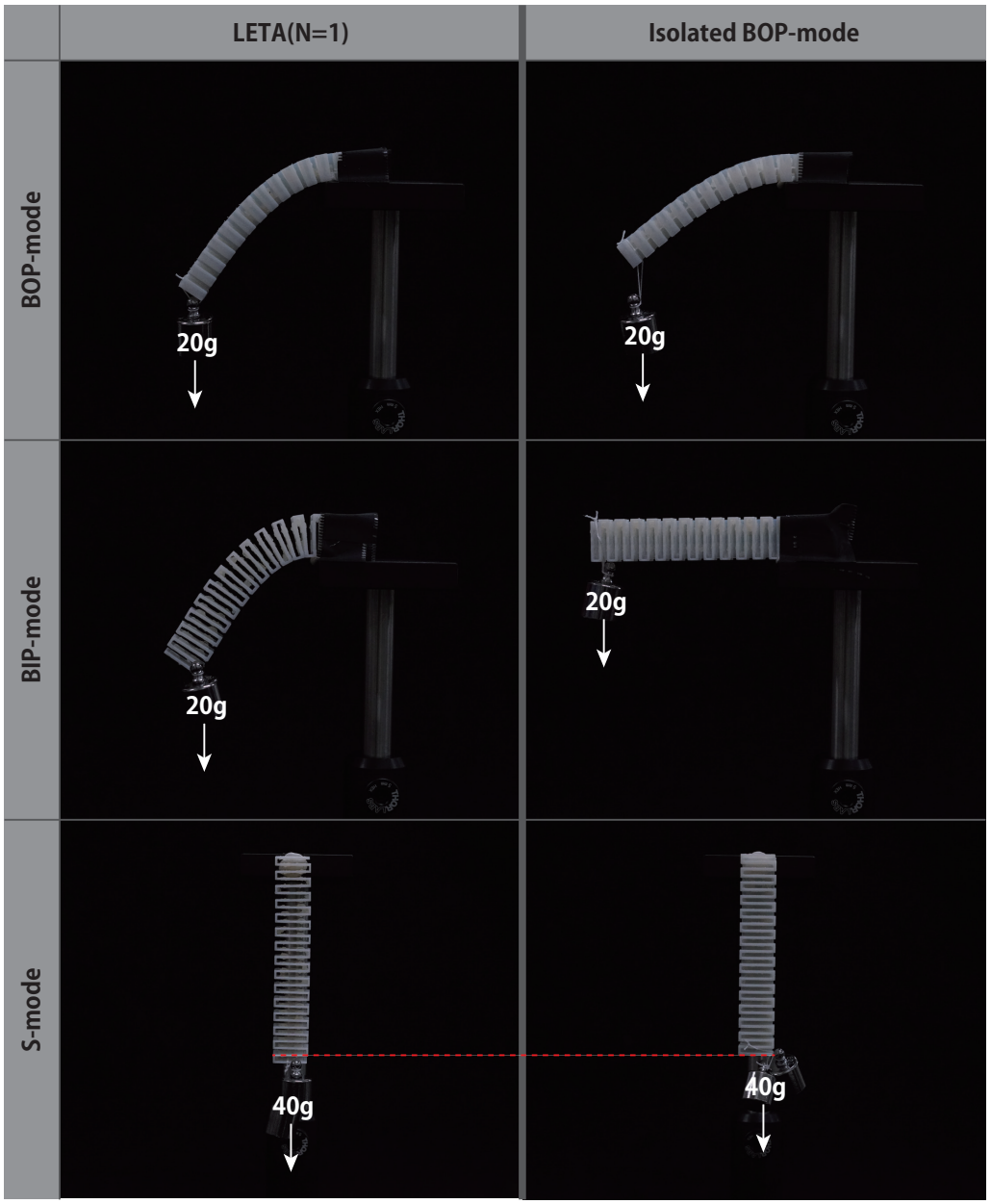

Figure 4.1: Measure of isolation characteristics.

4.2 Experiment2: Evaluation of control method

4.2.1 Purpose

The proposed soft manipulator uses an isolated structure that deforms reversibly from a planar structure only to a particular and only deformation shape. As described in Section 3.4, when ON/OFF control is applied to the proposed manipulator, only two of the curved shapes that the proposed manipulator can hold. Therefore, PID control is applied to retain the deformed shape in the state between transitions from the initial state to the equilibrium state. In Experiment 2, I confirm whether the PID control can be used to hold the proposed manipulator in the desired deformed state.

4.2.2 Evaluation conditions

Evaluated manipulator consists of the structure (the thickness of the local beam was 0.8mm, the length of the local beam was 14mm, the distance between the local beam was 3mm, the thickness of the structure was 10mm, the thickness of the thin shell was 0.25mm, and the number of local beams was into 30), the BMX with a length of 58mm and the flex sensor with a length of 112.24mm. It was driven by fixing the side where the metallic wires of the proposed manipulator came out and applying a current of 0.3A. As shown in Figure 4.2, when only ON/OFF control is performed, the values of the bending sensors are from the default value = 550 to the maximum value = 633. Therefore, PID control was carried out by setting the target values of bending sensors to two types, 580 and 610, between initial and maximum values. In this experiment, PID control parameters were controlled as $K_p = 1, K_i = 15, K_d = 4$.

4.2.3 Result

Figure 4.3 and Figure 4.4 show the results of the control. As can be seen from the diagram, it can be seen that the proposed manipulator holds its shapes while vibrating around the target values. It is assumed that the expansion operation is slower than the contraction operation because the expansion operation is performed by natural heat radiation, while the contraction operation of BMX is controlled by current flow. Therefore, it is considered that the delay of the feedback occurred and it vibrated near the target value.

It was also found that the time before reaching the target value can be changed by changing the value of the proportional gain of the PID control parameter (Figure 4.5). Proportional gain is a parameter that determines the manipulated variable in proportion to the control deviation. The larger the value of the proportional gain, the shorter the time that reaches the target value.

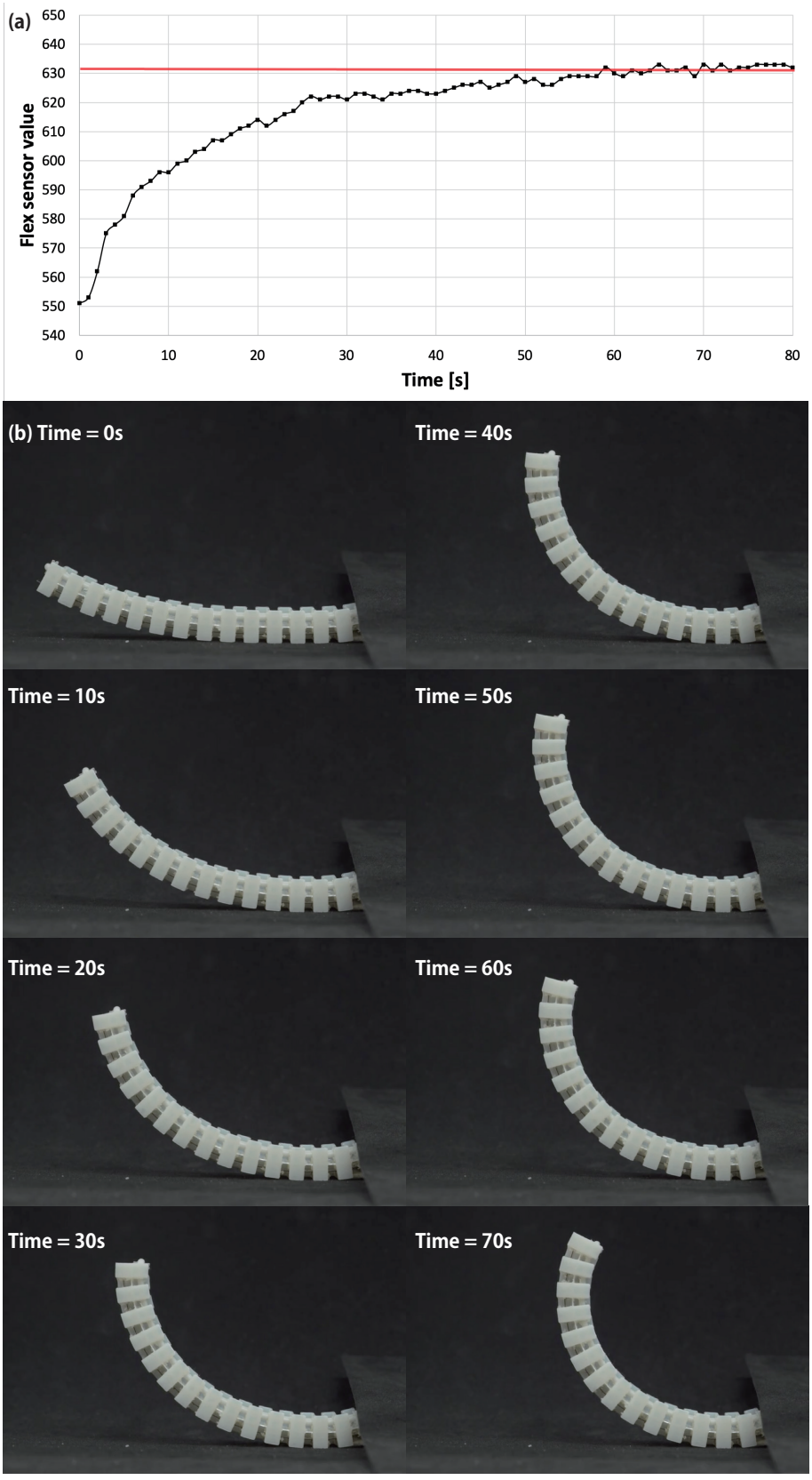

Figure 4.2: Result of ON/OFF control.

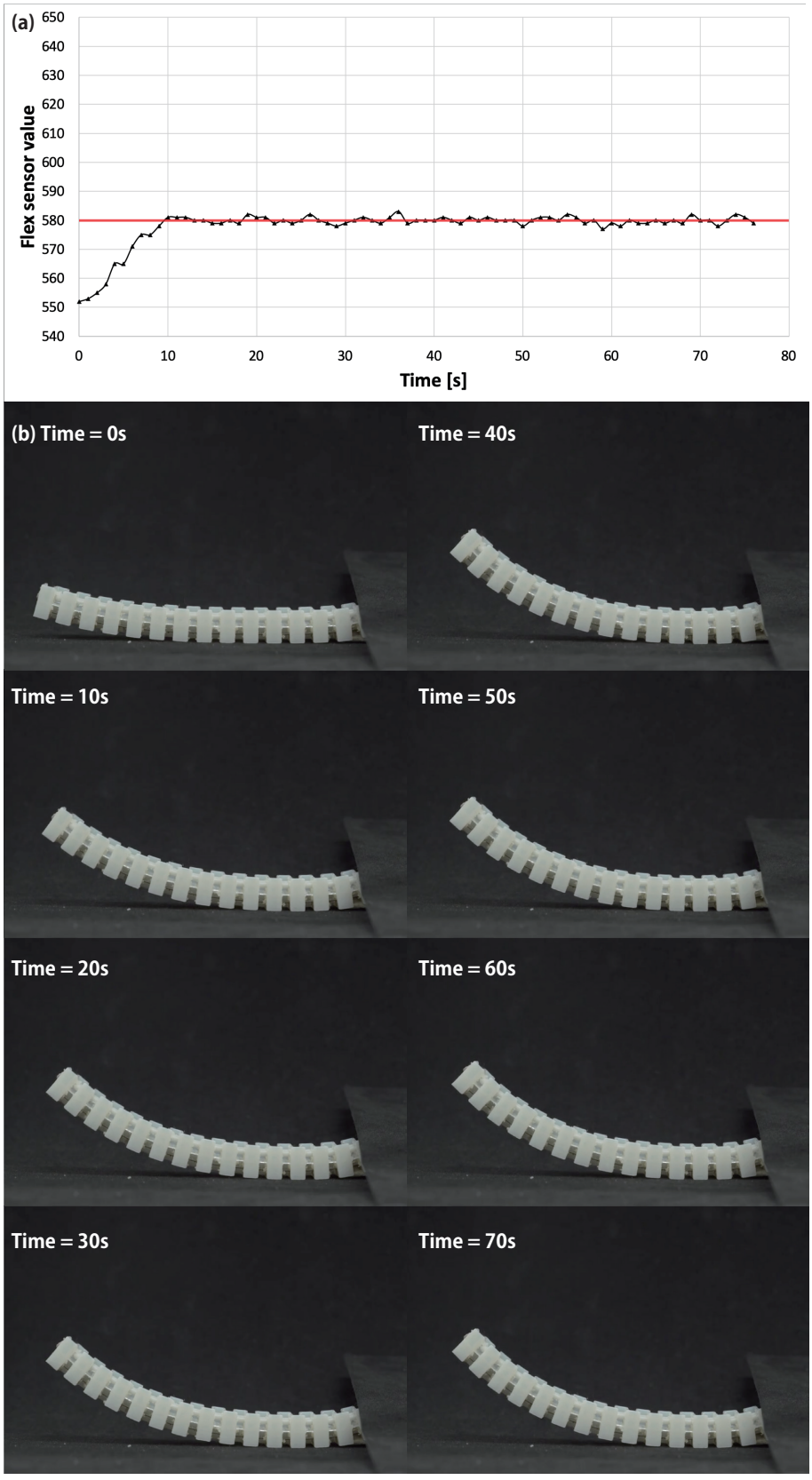

Figure 4.3: Result of PID control(target values = 580).

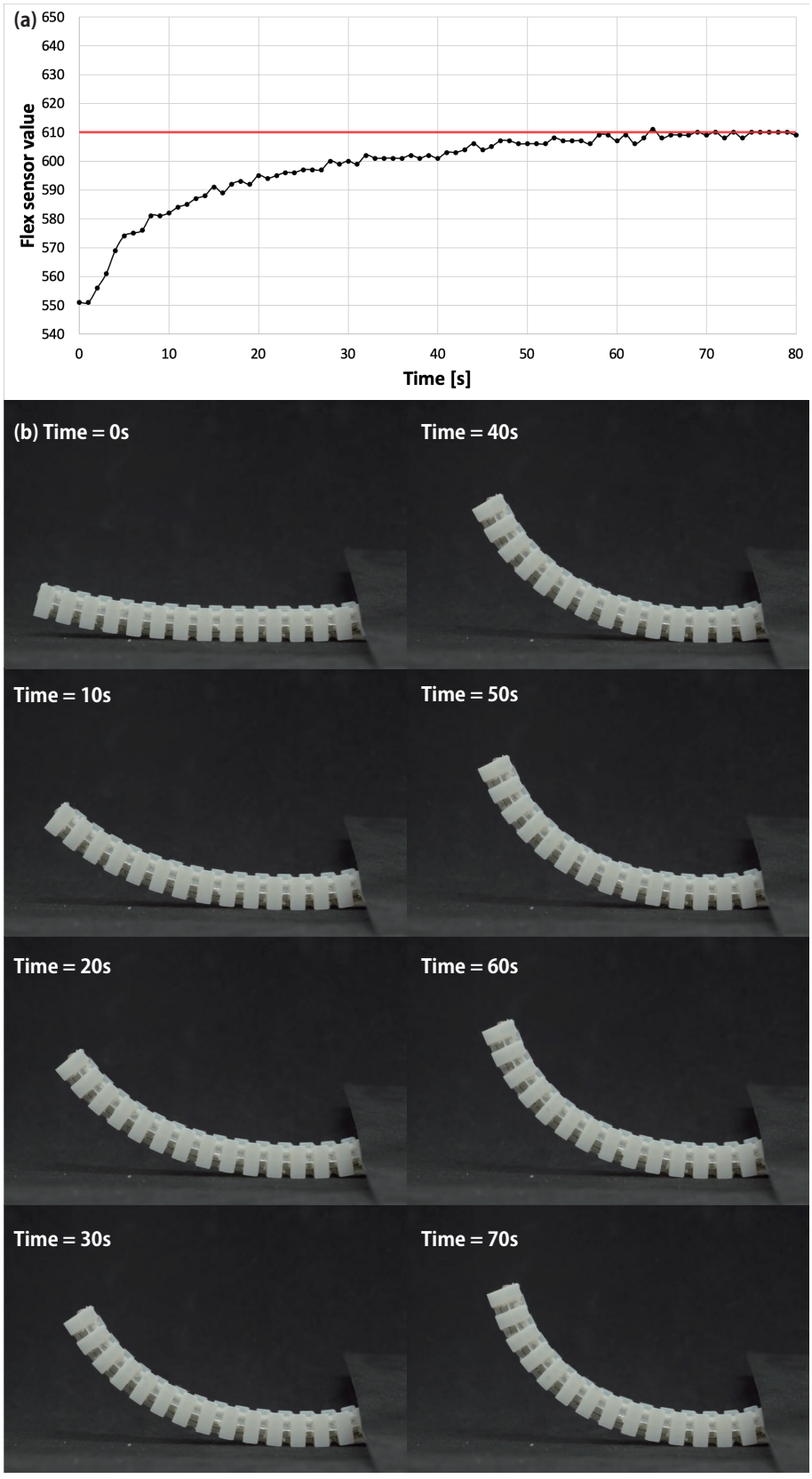

Figure 4.4: Result of PID control(target values = 610).

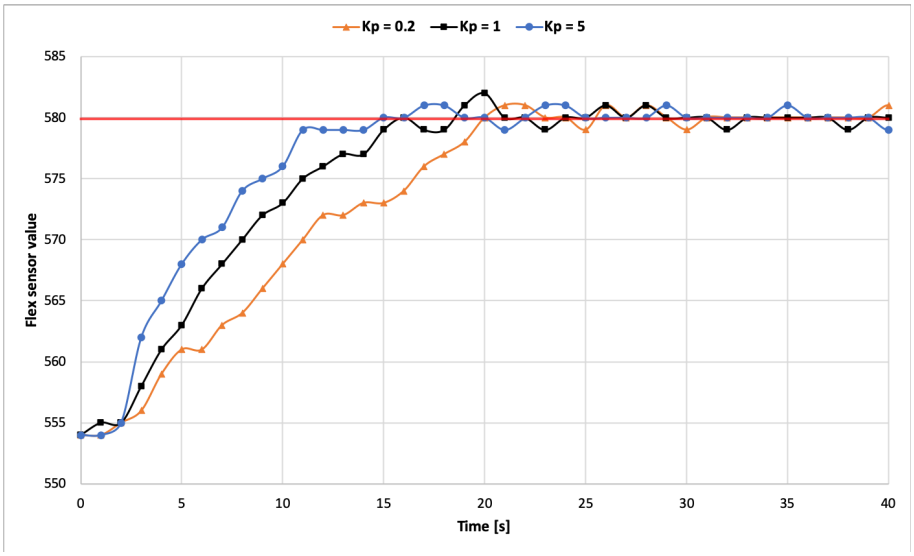

Figure 4.5: Result of changing proportional gain.

4.3 Experiment3: Evaluation of output force

4.3.1 Purpose

The proposed manipulator is driven by contracting the isolated structure with BMX. In Experiment 3, by measuring the maximum output force of the proposed manipulator and the maximum output force of the BMX itself used therein, I confirm how much the output of the BMX contributes to the output of the proposed manipulator.

4.3.2 Evaluation conditions

Evaluated manipulator consists of the structure (the thickness of the local beam was 0.8mm, the length of the local beam was 14mm, the distance between the local beam was 3mm, the thickness of the structure was 10mm, the thickness of the thin shell was 0.25mm, and the number of local beams was into 30), the BMX with a length of 58mm and the flex sensor with a length of 112.24mm. As a way of evaluation test, the lifting test of the weight is carried out for BMX of the same length as that used in the proposed manipulator and its interior.

The procedure of evaluation is as follows.

1. Fix one side of the proposed manipulator and BMX, and attach the weight to the other side
2. Apply a drive current of 0.3A
3. If the endpoint to which the weight was attached was raised to the initial position, it is considered that the weight was lifted completely, and repeat the operations 1 and 2 by adding a 10g weight

4.3.3 Result

Evaluation of the proposed manipulator is shown in Figure 4.6 and Evaluation of the BMX is shown in Figure 4.7, 4.8, 4.9, 4.10. The dashed red line in the figure represents the initial position before attaching the weight. The test results are also shown in Table 4.1.

As the results of the evaluation, the maximum output of the proposed manipulator was 10gf, and the maximum output of BMX alone was 30gf. For the isolated structures used, the output of the proposed manipulator became 1/3 of the output of the BMX. As a factor that the output of the proposed manipulator becomes smaller than the output of the BMX alone, it is considered that the energy is used for the deformation of the structure, the flex sensor and the silicon tubes constituting the proposed manipulator.

Table 4.1: Result of output load evaluation.

	10gf	**20gf**	**30gf**	**40gf**
Proposed manipulator	◯	×	-	-
BMX	◯	◯	◯	×

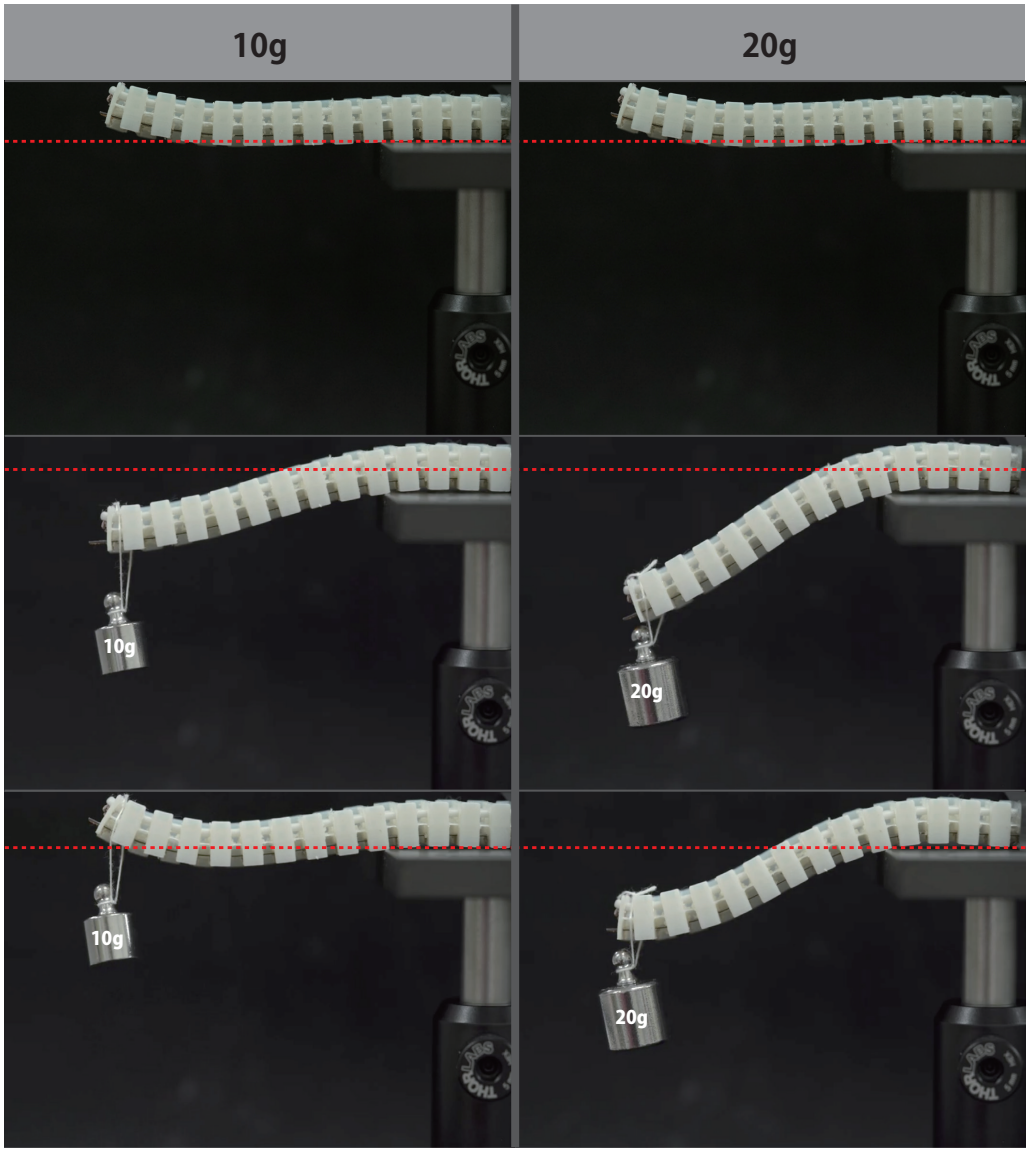

Figure 4.6: Experiment3 of proposed manipulator.

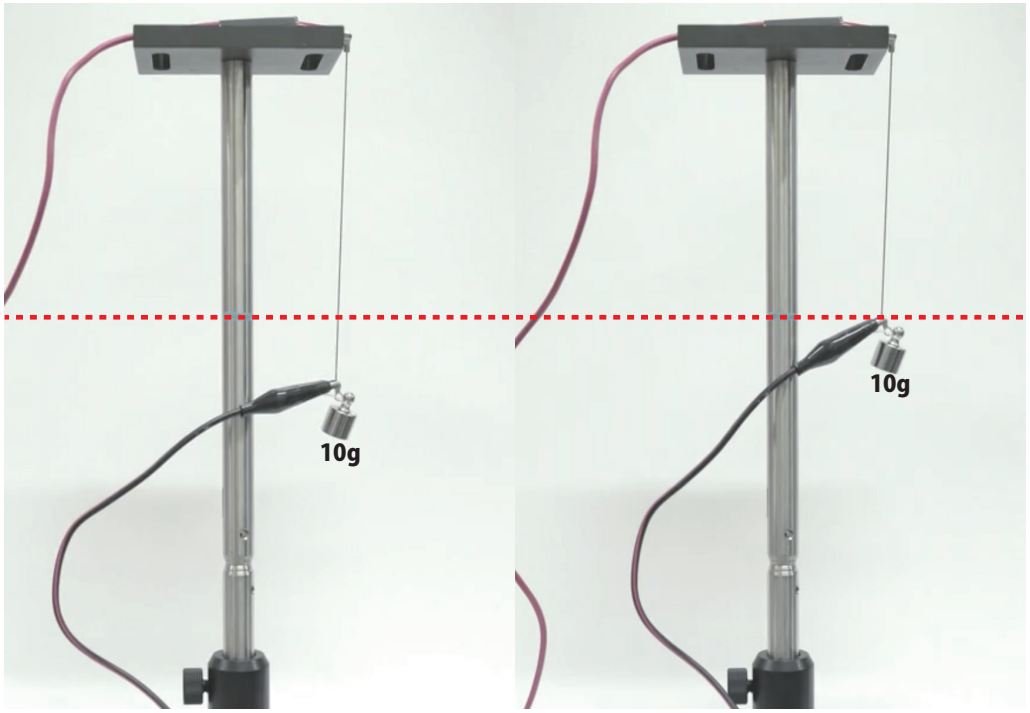

Figure 4.7: Experiment3 of BMX (weight = 10g).

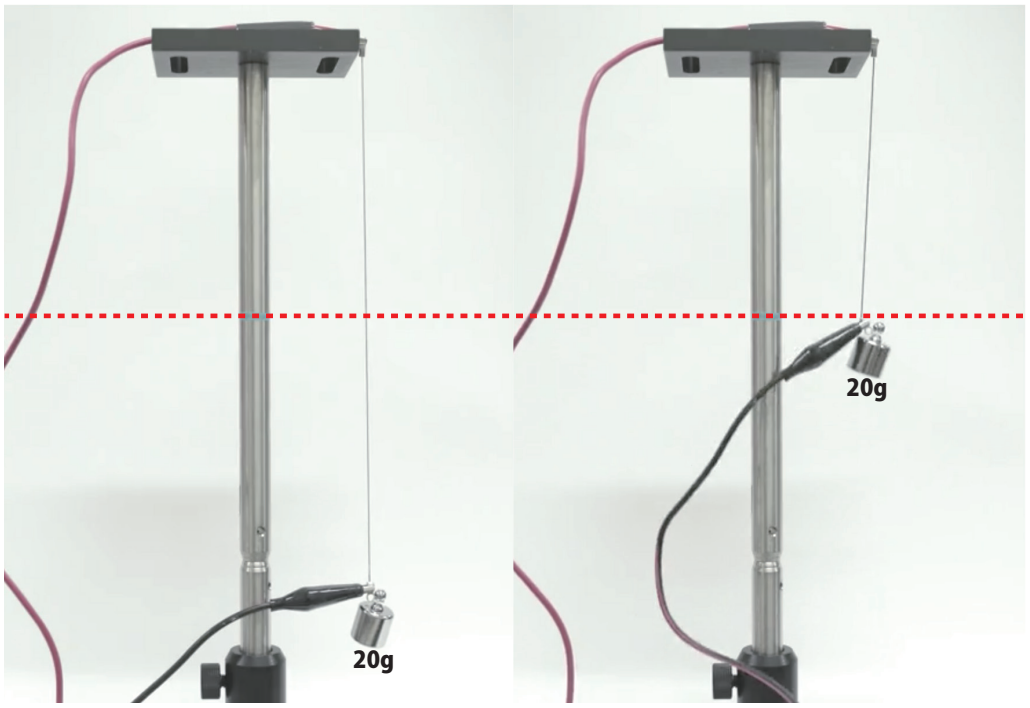

Figure 4.8: Experiment3 of BMX (weight = 20g).

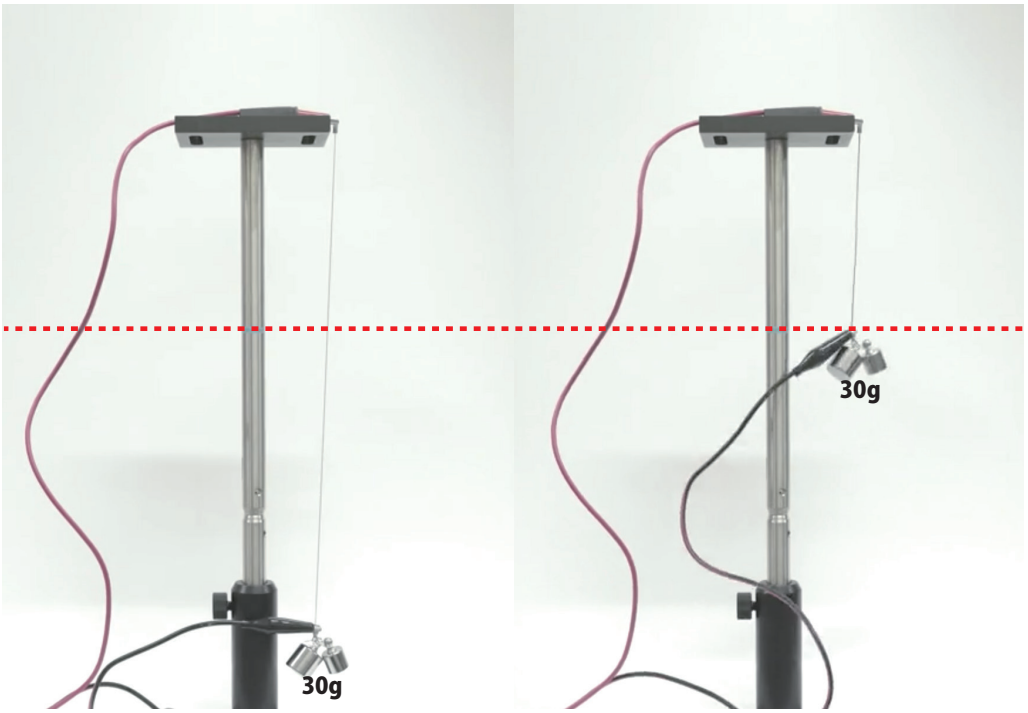

Figure 4.9: Experiment3 of BMX (weight = 30g).

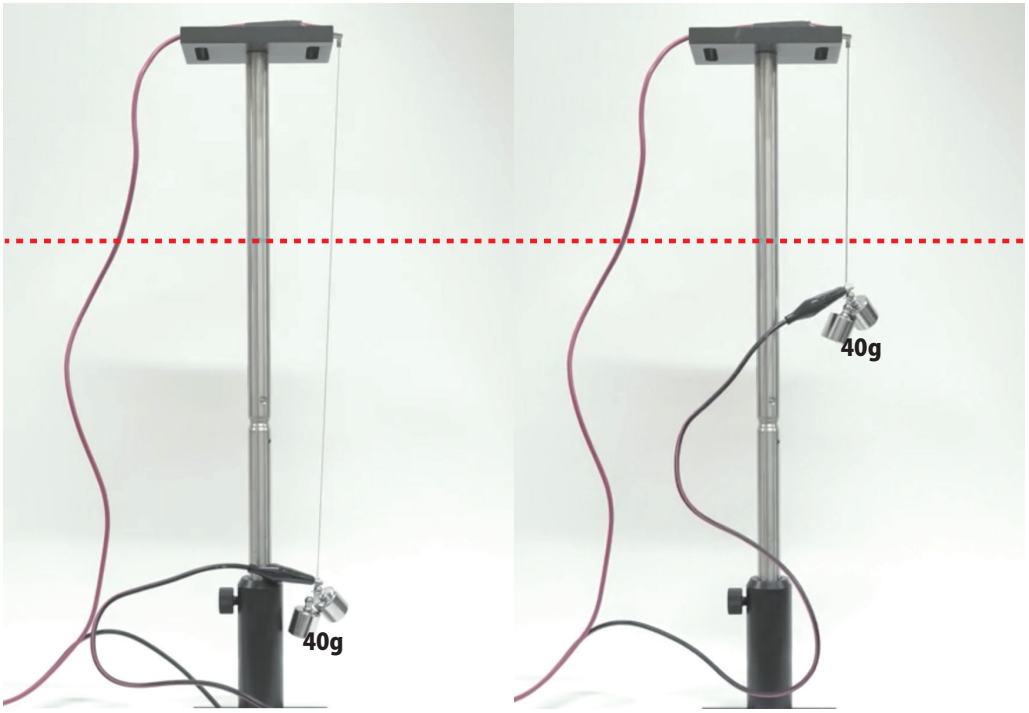

Figure 4.10: Experiment3 of BMX (weight = 40g).

Chapter 5

Application

5.1 Soft Manipulator

Since the proposed soft manipulator has compliance for isolated curve deformation, it is possible to grip objects of differing sizes (sponges of 40mm and 30mm in width) only by ON/OFF control. As shown in Figure 5.1, the proposed manipulator can grip the soft object without deforming it.

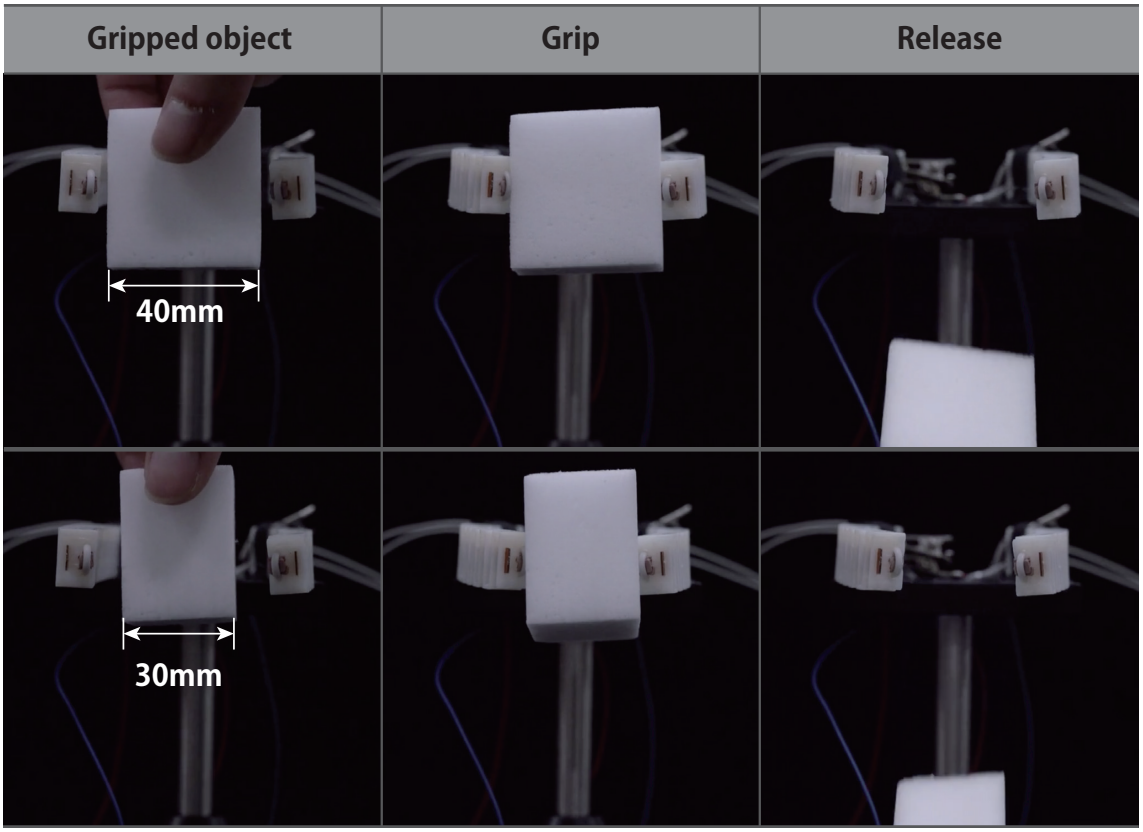

Figure 5.1: Soft Manipulator using proposed manipulator.

5.2 stuffed toy manipulator

The proposed soft manipulator is compliant for certain one deformations, but the material itself is hard. When a soft manipulator is used in an environment where people are on the side, the safety that does not cause injury with people when it comes into contact is required. For that purpose, the softness of the surface (energy absorption) is required. Therefore, by covering the outside of the proposed soft manipulator with flexible materials, the softness of the surfaces can be realized. In this study, I created the stuffed toy manipulator that guarantees the softness of surfaces by using a stuffed toy as an example of flexible materials and inserting the proposed manipulator inside the stuffed toy (Figure5.2).

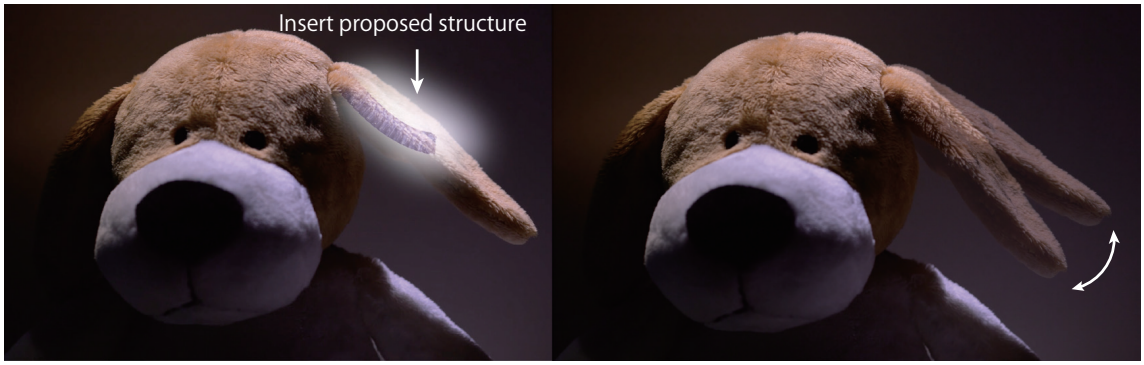

Figure 5.2: Stuffed toy manipulator.

5.3 The manipulator with the arbitrary outside shape

The proposed method is capable of creating manipulators with arbitrary outside shape. As shown in Figure 5.3, by taking a Boolean product of a 3D model with a desired outside shape and the isolated structure, the isolated structure of the desired outside shape can be created.

A number of soft manipulators proposed in previous studies were manufactured using soft lithography as a manufacturing technique. Therefore, in order to make the soft manipulator of the arbitrary outside type, it was necessary to make the mold die matching to the outside type. On the other hand, since the technique of this study manufactures structures using a 3D printer, an arbitrary outside type manipulator can be manufactured with fewer steps than conventional methods.

Figure 5.4 shows the manipulator of armadillo arm shape.

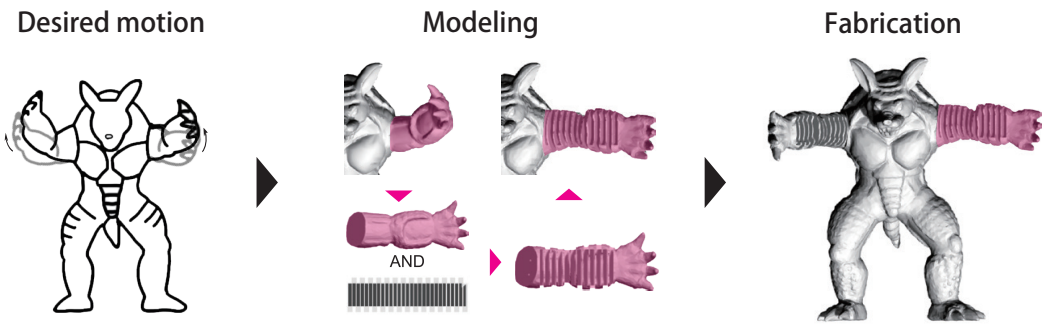

Figure 5.3: Design method of proposed manipulator that desired shape.

Figure 5.4: The manipulator of armadillo arm shape.

Chapter 6

Future work

6.1 Treatment of Heat Generated During Actuation

SMA generates heat during deformation motion. This becomes a large factor which melts the 3D printed structure and destroys the structure when the proposed manipulator continues to move for a long time. In order to solve this issue, this study enhances heat dissipation by inserting SMAs through silicon tubes and then into the interior of 3D printed structures. However, there are limitations to this approach and long-term use of the proposed manipulator ultimately leads to structural fracture (Figure6.1). Therefore, the examination of more efficient heat radiation technique in the actuation is an important subject in the future.

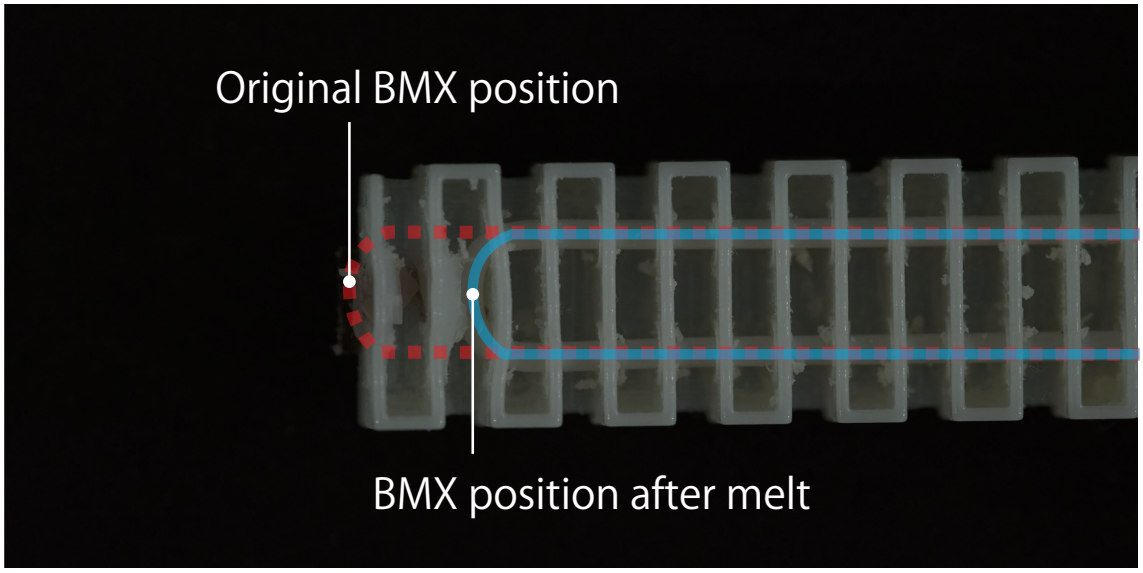

Figure 6.1: Structure melted by driving heat.

6.2 Output force

From the experimental result of Section 5.3, the force of the actuation by BMX used at present was about 10gf. Applications that can be applied to current outputs include lifting light objects and representing motion as shown in Chapter 4. On the other hand, there are many applications for soft manipulators and soft actuators, such as lifting heavier objects or

providing human power assist, which requires larger output than the current ones. Therefore, the examination of the actuation technique with stronger output, such as SMA with stronger output than BMX and linear actuation by winding the thread instead of SMA, is also pointed out as a future problem.

6.3 3D Printing Materials and Methods

The proposed structures were isolated by inserting a thin shell into the interior of the conventional LETA (N=1) structure. Initially, I used Form2 photocuring resins to make this construction. However, thin shell, empirically, changed the elastic modulus of the material in a few weeks from printing, and fracture occurred during actuation. This may be attributed to the fact that the light-curing resin proceeded further hardening in environmental light after printing and the material deteriorated. I used Stratasis's photocurable acrylic resins and Ultimaker's PLA to print the same structure and found that the fragility was improved. In other words, the vulnerability of thin shells depends on the substrate used for 3D printing and the printing technique. Therefore, further examination of printing substrates and printing techniques used for the proposed manipulator as future work will be given.

Chapter 7

Conclusion

In this study, I created a soft manipulator that can accurately measure the deformation state while keeping the compliance which can flexibly correspond even to the unknown object. In order to create this manipulator, I proposed a structure that deforms reversibly only from a planar state to a specific and only one curved deformation state. The proposed structure is compliant for specific and only deformation and stiff for other deformations. In this study, this property regard as "isolation" of deformation. It is realized by improving Lamina emergent torsion array (LETA) structure in order to realize the proposed structures. LETA is a structure in which curved deformation is realized by putting a cut pattern of parallel in hard material. However, it is also known that the LETA undergoes stretching and twisting deformation in addition to the bending deformation. Therefore, in the proposed structure, the deformation is isolated only by the curved deformation by inserting a thin shell in the neutral plane of the LEAT structure. By creating a soft manipulator using the structure isolated only for curved deformation, the deformation shape of a specific time can be measured accurately using a flex sensor, which is an element to measure bending. Additionally, since the deformation of the structure is isolated, the proposed manipulator can be driven using a shape memory alloy with simple expansion and contraction movement.

In addition, in order to evaluate the performance of the proposed soft manipulator, evaluation of the isolated property, evaluation of the control performance and evaluation experiments of output force were carried out. In the evaluation experiment of the isolation property, it was shown that the proposed structure was isolated even in a real environment by attaching a weight on the structure. In the evaluation experiment of the control performance, PID control which adjusts the amount of current applied to the shape memory alloy was carried out using the shape of specific time measured by the flex sensor as a feedback value, and it was evaluated whether the desired shape can be held. In the evaluation experiments of output load, the maximum power of the proposed manipulator and the maximum power of the shape-memory alloys were measured and compared. Finally, three applications ware proposed to show the usefulness of proposed manipulator.

Acknowledgement

First and foremost, I would like to express my heartfelt gratitude to Prof. Yoichi Ochiai, Prof. Takahito Aoto, and Taisuke Ohshima for support and encouragement, which are indispensable to me to complete my master thesis. Having met Prof. Ochiai in my undergraduate days and having been able to spend exciting days at DNG for four years is a treasure of my life. I was on the brink of being discouraged many times, but because of the support from Prof. Aoto, I was able to overcome it.

I am grateful to acknowledge the members, ex-members and staff from the DNG. It was such a great pleasure for me to meet them.

Last, my sincerest thanks go to my family. Their encourage always support me. Thank you.

References

[1] Rolf Pfeifer, Max Lungarella, and Fumiya Iida. The challenges ahead for bio-inspired 'soft' robotics. *Communications of the ACM*, Vol. 55, No. 11, pp. 76–87, 2012.

[2] Raphael Deimel and Oliver Brock. A Novel Type of Compliant, Underactuated Robotic Hand for Dexterous Grasping. *The International Journal of Robotics Research*, Vol. 35, No. 1-3, pp. 161–185, 2016.

[3] Nadia G. Cheng, Maxim B. Lobovsky, Steven J. Keating, Adam M. Setapen, Katy I. Gero, Anette E. Hosoi, and Karl D. Iagnemma. Design and analysis of a robust, low-cost, highly articulated manipulator enabled by jamming of granular media. *Proceedings - IEEE International Conference on Robotics and Automation*, pp. 4328–4333, 2012.

[4] FANUC CORPORATION. Lerge Size Robot. `https://www.fanuc.co.jp/en/product/robot/model/index.html,(2020-1-8)`.

[5] GIMATIC S.r.l. PARALLEL GRIPPERS. `https://shop.gimatic.com/en/parallel-grippers,(2020-1-8)`.

[6] UFACTORY. UARM SWIFT PRO. `https://www.ufactory.cc/#/en/uarmswift,(2020-1-8)`.

[7] Thingiverse. MeArm. `https://www.thingiverse.com/thing:993759,(2020-1-8)`.

[8] Raphael Deimel and Oliver Brock. A compliant hand based on a novel pneumatic actuator. *Proceedings - IEEE International Conference on Robotics and Automation*, pp. 2047–2053, 2013.

[9] Filip Ilievski, Aaron D. Mazzeo, Robert F. Shepherd, Xin Chen, and George M. Whitesides. Soft robotics for chemists. *Angewandte Chemie - International Edition*, Vol. 50, No. 8, pp. 1890–1895, 2011.

[10] Cianchetti Matteo, Follador Maurizio, Mazzolai Barbara, Dario Paolo, and Laschi Cecilia. Design and development of a soft robotic octopus arm exploiting embodied intelligence. *Proceedings - IEEE International Conference on Robotics and Automation*, pp. 5271–5276, 2012.

[11] Hu Jin, Erbao Dong, Min Xu, Chunshan Liu, Gursel Alici, and Yang Jie. Soft and smart modular structures actuated by shape memory alloy (SMA) wires as tentacles of soft robots. *Smart Materials and Structures*, Vol. 25, No. 8, pp. 1–10, 2016.

[12] Hugo Rodrigue, Wei Wang, Dong Ryul Kim, and Sung Hoon Ahn. Curved shape memory alloy-based soft actuators and application to soft gripper. *Composite Structures*, Vol. 176, No. November, pp. 398–406, 2017.

[13] Robert F. Shepherd, Adam A. Stokes, Rui M.D. Nunes, and George M. Whitesides. Soft machines that are resistant to puncture and that self seal. *Advanced Materials*, Vol. 25, No. 46, pp. 6709–6713, 2013.

[14] Eric Brown, Nicholas Rodenberg, John Amend, Annan Mozeika, Erik Steltz, Mitchell R. Zakin, Hod Lipson, and Heinrich M. Jaeger. Universal robotic gripper based on the jamming of granular material. *Proceedings of the National Academy of Sciences of the United States of America*, Vol. 107, No. 44, pp. 18809–18814, 2010.

[15] Jun Shintake, Samuel Rosset, Bryan Schubert, Dario Floreano, and Herbert Shea. Versatile Soft Grippers with Intrinsic Electroadhesion Based on Multifunctional Polymer Actuators. *Advanced Materials*, Vol. 28, No. 2, pp. 231–238, 2016.

[16] Andrew D. Marchese, Cagdas D. Onal, and Daniela Rus. Autonomous Soft Robotic Fish Capable of Escape Maneuvers Using Fluidic Elastomer Actuators. *Soft Robotics*, Vol. 1, No. 1, pp. 75–87, 2014.

[17] Ming Xu, Zhaoyan Cui, Zhongfan Chen, and Jinhua Xiang. Design and Control of a Soft and Continuously Deformable 2D Robotic Manipulation System. *IEEE International Conference on Robotics and Automation, 2014. Proceedings. ICRA '14. 2014*, Vol. 42, No. 7, pp. 750–759, 2014.

[18] Daekwon Park, Juhun Lee, and Alejandra Romo. Poisson's ratio material distributions: Variable Poisson's ratio material systems for adaptive building applications. *CAADRIA 2015 - 20th International Conference on Computer-Aided Architectural Design Research in Asia: Emerging Experiences in the Past, Present and Future of Digital Architecture*, pp. 735–744, 2015.

[19] Yong Lae Park, Bor Rong Chen, and Robert J. Wood. Design and fabrication of soft artificial skin using embedded microchannels and liquid conductors. *IEEE Sensors Journal*, Vol. 12, No. 8, pp. 2711–2718, 2012.

[20] Edward L. White, Michelle C. Yuen, Jennifer C. Case, and Rebecca K. Kramer. Low-Cost, Facile, and Scalable Manufacturing of Capacitive Sensors for Soft Systems. *Advanced Materials Technologies*, Vol. 2, No. 9, pp. 1–10, 2017.

[21] Selim Ozel, Erik H. Skorina, Ming Luo, Weijia Tao, Fuchen Chen, Yixiao Pan, and Cagdas D. Onal. A composite soft bending actuation module with integrated curvature sensing. *Proceedings - IEEE International Conference on Robotics and Automation*, Vol. 2016-June, pp. 4963–4968, 2016.

[22] Graham Pitcher. A helping hand. *New Electronics*, Vol. 49, No. 10, pp. 12–14, 2016.

[23] Bianca S. Homberg, Robert K. Katzschmann, Mehmet R. Dogar, and Daniela Rus. Haptic identification of objects using a modular soft robotic gripper. *IEEE International Conference on Intelligent Robots and Systems*, Vol. 2015-Decem, pp. 1698–1705, 2015.

[24] Taisuke Ohshima, Tomohiro Tachi, Hiroya Tanaka, and Yasushi Yamaguchi. Analysis and design of elastic materials formed using 2D repetitive slit pattern. *Proceeding - International Association for Shell and Spatial Structures Symposium*, No. August, pp. IASS2015–526418:1–12, 2015.

[25] Julian Panetta, Qingnan Zhou, Luigi Malomo, Nico Pietroni, Paolo Cignoni, and Denis Zorin. Elastic textures for additive fabrication. *ACM Transactions on Graphics*, Vol. 34, No. 4, pp. 1–12, 2015.

[26] Christian Schumacher, Bernd Bickel, Jan Rys, Steve Marschner, Chiara Daraio, and Markus Gross. Microstructures to control elasticity in 3D printing. *ACM Transactions on Graphics*, Vol. 34, No. 4, pp. 1–13, 2015.

[27] Jonàs Martínez, Jérémie Dumas, and Sylvain Lefebvre. Procedural voronoi foams for additive manufacturing. *ACM Transactionson Graphics*, Vol. 35, No. 4, pp. 44:1–44:12, 2016.

[28] Alexandra Ion, Ludwig Wall, Robert Kovacs, and Patrick Baudisch. Digital mechanical metamaterials. *Conference on Human Factors in Computing Systems - Proceedings*, Vol. 2017-May, pp. 977–988, 2017.

[29] Alexandra Ion, Johannes Frohnhofen, Ludwig Wall, Robert Kovacs, Mirela Alistar, Jack Lindsay, Pedro Lopes, Hsiang Ting Chen, and Patrick Baudisch. Metamaterial mechanisms. *UIST 2016 - Proceedings of the 29th Annual Symposium on User Interface Software and Technology*, pp. 529–539, 2016.

[30] Evgueni T. Filipov, Tomohiro Tachi, Glaucio H. Paulino, and David A. Weitz. Origami tubes assembled into stiff, yet reconfigurable structures and metamaterials. *Proceedings of the National Academy of Sciences of the United States of America*, Vol. 112, No. 40, pp. 12321–12326, 2015.

[31] Roberto Naboni and Lorenzo Mirante. Metamaterial computation and fabrication of auxetic patterns for architecture. *Blucher Design Proceedings*, Vol. 2, No. 3, pp. 129–136, 2015.

[32] Pibo Ma. A Review on Auxetic Textile Structures, Their Mechanism and Properties. *Journal of Textile Science & Fashion Technology*, Vol. 2, No. 1, pp. 1–10, 2019.

[33] Yasushi Yamaguchi, Tomohiro Tachi, Taisuke Ohshima. Japan patent JP2019-23489A(2019.02.14).

[34] Todd G. Nelson, Robert J. Lang, Nathan A. Pehrson, Spencer P. Magleby, and Larry L. Howell. Facilitating deployable mechanisms and structures via developable lamina emergent arrays. *Journal of Mechanisms and Robotics*, Vol. 8, No. 3, 2016.

[35] Bryce P. DeFigueiredo, Trent K. Zimmerman, Brian D. Russell, and Larry L. Howell. Regional Stiffness Reduction Using Lamina Emergent Torsional Joints for Flexible Printed Circuit Board Design. *Journal of Electronic Packaging, Transactions of the ASME*, Vol. 140, No. 4, 2018.

[36] dukta GmbH. dukta. `https://dukta.com,(2020-1-8)`.

[37] Joseph O. Jacobsen, Brian G. Winder, Larry L. Howell, and Spencer P. Magleby. Lamina emergent mechanisms and their basic elements. *Journal of Mechanisms and Robotics*, Vol. 2, No. 1, pp. 1–9, 2010.

[38] Hayato Togawa. *Yugenyousohouniyoru Shindoukaiseki*. Tokyo: Science-sha, 1975.

[39] TOKI CORPORATION. BioMetal Helix. `https://www.toki.co.jp/biometal/english/contents.php,(2020-1-8)`.

[40] Spectra Symbol. RESISTIVE FLEX SENSORS 3.75inch. `https://www.spectrasymbol.com/product/flex-sensors/,(2020-1-8)`.